SEMI-ANNUAL REPORT

RESEARCH ON HOLLOW CATHODES IN MERCURY ION THRUSTERS

CONTRACT NO. 952685

JET PROPULSION LABORATORY

CALIFORNIA INSTITUTE OF TECHNOLOGY

This work was performed for the Jet Propulsion Laboratory, California Institute of Technology, sponsored by the National Aeronautics and Space Administration under Contract NAS7-100.

REPORT NO. 14

SPACE PROPULSION PROGRAM

COLLEGE OF ENGINEERING

COLORADO STATE UNIVERSITY

FORT COLLINS, COLORADO

SEMI-ANNUAL REPORT

for

CONTRACT NO. 952685

prepared for

JET PROPULSION LABORATORY

CALIFORNIA INSTITUTE OF TECHNOLOGY

March, 1970

Technical Management

Mr. Eugene Pawlik
Jet Propulsion Laboratory
Pasadena, California

Principal Investigator

Mr. William R. Mickelsen
Professor of Mechanical Engineering
Colorado State University
Fort Collins, Colorado

Associate Investigator

Dr. Giuseppe Palumbo
Research Associate
Colorado State University
Fort Collins, Colorado

CONTENTS

EFFECT OF OPERATING PARAMETERS ON PERFORMANCE OF STANDARD THRUSTER

by G. Palumbo and R. Vahrenkamp*

In an effort to improve thruster performance by the reduction of discharge and impingement losses, the effects of grid spacing, accelerator potential, cathode flow rate, and main magnetic field intensity were considered. Through an investigation of these parameters, a base operating condition has been established.

The interrelation of grid spacing, magnetic field, and accelerator potential was determined by a variation of these parameters at a constant main and cathode flow of 6.1 and 0.7 gm/hr respectively. The keeper current was held constant at 0.1 amperes.

Because of warpage, an exact measure of grid spacing was difficult to achieve with an ordinary feeler gauge. However, knowing the location and the amount of the warpage of each grid, a reasonable spacing could be obtained. The range of spacing was from .045 in. to .085 in. The magnet current, ranging from 0.1 to 3.0 amps, was varied at each grid spacing, as was the accelerator potential which ranged from 1.0 to 2.0 kilovolts.

Apparatus

Descriptions of the vacuum facility and experimental apparatus have been reported previously[1]; here the concern is mainly in describing the changes that were made in order to facilitate the research and to improve the reliability of the data. The keeper has been changed from the original

---

*Graduate Research Assistant, Master of Science Student

loop of thermocouple wire to a rectangular strip of refractory metal with a central hole. The advantages of this new keeper are due to the exact location of the hole with respect to the cathode tip and improved resistance to melting. The circuitry was simplified by eliminating the starter supply so that there is no need for the diode in series with the low voltage keeper supply.

The cathode remains unchanged, but its vaporizer heater was moved 10 cm. further back in order to prevent heating of the vaporizer by the cathode heater. Subsequent instability and difficulty in operating the thruster, probably due to vapor condensation in the pipe between the heater and the cathode, forced relocation of the heater to its former position. This action corrected the instabilities.

The feed system was also improved by adding a reservoir and valve for each feed line so that the refilling could be accomplished during engine operation without turning off the high voltage. This procedure ensures versatility and safety.

The instrumentation has been improved by using a digital voltmeter (D.V.M.) to measure voltage and current for the arc and magnet. A separate D.V.M. is being used to measure beam and impingement current. Each D.V.M. has been calibrated against a calibrated power supply driving a precision resistor. The currents are measured through the voltage drop across a precision resistor of 1 ohm, so that the reading in voltage is equivalent to the current.

An oscilloscope is used to monitor the arc current in order to observe fluctuations in the discharge. The D.V.M. for the arc, and magnet measurements, and the oscilloscope are isolated from ground and located in a cabinet protected from the operator's side by a lucite door.

A switch located in the same cabinet can be used to connect signals from the arc variables, keeper, and magnet across the D.V.M. In addition, all these can be visualized on the scope so as to isolate the source of instability.

Effect of Grid Spacing

The effect of grid spacing on discharge ev/ion is shown in Figures 1 and 2 as a function of magnet current and of accelerator voltage. Data collected at a grid spacing of .045-in are not presented because of considerable instabilities at this spacing which preclude operation above a mass utilization of 85%. The effect of grid spacing, at various voltages, on impingement was then investigated. The results are shown in Figure 3.

From the data reported here on the effect of grid spacing, it is evident that there is a significant decrease in discharge losses at the closer grid spacings. However, the impingement seems to be relatively unaffected by grid spacing. It is believed that the vacuum tank pressure is responsible for this, since it is somewhat high in the bell jar. Gauge measurements in the tank indicate about 1×10^{-5} torr, while "upstream" of the thruster, the gauge reading indicates a pressure of 7×10^{-5} torr. At the accelerator electrodes, the pressure is probably intermediate to these two extremes.

The limit of closest operational grid spacing (0.055 inch) is also assumed to be a function of this pressure.

Effect of Accelerator Voltage

Discharge losses for several sets of accelerator voltages are shown in Figure 4. From these data it is clear that discharge losses are significantly reduced for the greater accelerator voltages.

Effect of Total Flow Rate at Standard Base Operating Conditions

From the foregoing data, the following base condition for future thruster research was established:

1) The high voltage would be maintained at ±2 KV.

2) The magnet would be in the 1.7-2.0 amp range. This allows a wider range of mass utilization to be obtained, without a significant effect on thruster performance.

3) The grid spacing would be .060 in. This was chosen mainly for stability reasons, since excessive arcing was occuring at the closer spacings.

The effect of total flow rate, at these base conditions, was then determined and the results are shown in Figures 5 and 6. In obtaining these data, both the cathode and main flows were adjusted so that a constant discharge voltage of approximately 35 volts was maintained. Any increase in main flow resulted in a decrease of cathode flow.

Discussion

It is evident from Figures 1 and 2 that the performance is increased by decreasing the spacing. The distance and voltage difference between the screen grid and the accelerator grid set the field strength and the penetration of the same in the main discharge chamber. Such penetration effects the extraction surface for the ion and the focusing of the same out of the chamber.

Increasing the field strength by either increasing the high voltage or simply by reducing the spacing at a given voltage will result in an increase of the electric field strength, and as a consequence a deeper field penetration and an increase of ion extraction surface area. This will result in a higher beam current and decrease of discharge losses. This trend will be effective up to a point beyond which other detrimental effects will be important, such as increased accelerator current. The sudden increase of ev/ion below the 0.055-inch spacing, and the instability in the running condition, suggest that at the operating pressure the

break-down voltage could be reached at which a discharge could be set up between the two grids.

The effect of magnet current is closely related to the Larmor radius of the electrons and to diffusion and instability effects. By increasing the magnet current, the field strength increases, the Larmor radius decreases, and thus by confining the electrons closer to a field line more collisions will occur and thus will have as a consequence a longer path length from cathode to anode. The increase of collisions will increase the probability of ionization in the chamber and this will result in a higher ion density so that at the same arc power higher beam current can be extracted. The discharge losses will decrease because the ratio arc-power/beam-current will go down. When the electrons have had enough collisions to lose all their energy before reaching the anode, a further increase of field strength will not improve the probability of ionization, and will only increase the possibility of plasma instability. Plasma instability will increase diffusion of electrons to the anode thereby decreasing ionization probability, and an increase of discharge losses will result.

The major effect of increasing the total flow rate is in the increase of neutral density in the chamber, and thus higher rate of ionization. This will increase the ion density and a higher beam-current will result at the same arc power. As a consequence, the discharge losses will decrease and the performance will increase.

Conclusions

The main conclusions from this portion of the investigation are:

1) There is a significant decrease in discharge losses at the closer grid spacings.

2) There is an optimum magnet current, as far as discharge losses are concerned, but after a certain current is reached there is little effect over a wide range.

3) In the range investigated, increased total flow rate tended to increase the performance.

CONICAL BAFFLE

by R. Vahrenkamp and G. Palumbo

The importance of the baffle is to separate the two discharge regions that control the thruster performance. The open area is the most important part of the baffle region because it influences the impedence of the connection between the cathode discharge and the main discharge which controls the voltage drop through which the primary electrons are accelerated. The voltage at the baffle exit gives the energy to the electron, thereby controlling the amount of ionization in the main discharge.

Little has been done in the present study on the effect of the baffle open area; attention has been concentrated on the use of a conical baffle instead of the flat one. The intent of the conical baffle was to decrease the neutral atom density within the hollow-cathode discharge region by reducing the resistance to flow of neutrals leaving the pole piece interior.

Figure 7 is a sketch of the conical baffle configuration used in the tests. The conical baffle was designed to present the same open area to the discharge as the flat baffle used in earlier tests.

The effect of baffle geometry is summarized in Figure 8 where typical data obtained with a flat baffle and the conical one are compared. It appears from these data that the increased surface area of the conical baffle causes degradation in performance that exceeds any improvement which may be realized because of the geometric effect mentioned earlier.

EFFECT OF POLE PIECE GEOMETRY AND FIELDS ON PERFORMANCE

by G. Palumbo, R. Vahrenkamp, H.R. Kaufman*, P. Wilbur†, and W.R. Mickelsen

In the following sections a detailed description of the studies conducted on the inside region of the pole piece will be given. It is well known that significant increases in discharge losses result from replacing an oxide cathode with a hollow cathode in an electron-bombardment ion thruster. It has been suggested that this increase is due to an excessive ion flux to the inside walls of the pole piece region (ref. 2). Several attempts to decrease these losses will be described.

The changes made to the hollow cathode region include changes in the volume of the discharge region and magnetic and electric fields. The physical geometry of the pole piece, cathode and keeper were not altered. Preliminary investigation of the effect of a magnetic field inside the pole piece has been reported (ref. 3), and another similar investigation is being conducted elsewhere (ref. 4).

Simple Solenoid

An improvement was made to the pole piece region by changing the magnetic configuration inside by applying an internal magnetic field thereby reducing electron migration to the walls. It was presumed that the changes in the ion-drift electric field caused by reduction of the electron current to the walls would in turn reduce the ion wall flux, in a manner similar to that observed in the main chamber.

---

*doctoral candidate

†Assistant Professor of Mechanical Engineering

The internal field was applied by the use of a 21-turn solenoid winding of diameter close to the pole piece diameter as shown in Figure 9. When the current in the cathode pole piece coil is such that its field opposes the main field, the field configuration of Figure 10 was obtained. Performance data are presented in Figure 11. The data show a decrease in discharge losses as the cathode field is increased. For convenience, the effect of such a field on performance at 90% mass utilization is given in Figure 12, while Figure 13 shows the effect of the field on discharge voltage and beam current.

When the cathode-pole-piece coil is carrying a current in such a direction as to aid the main field in the cathode pole piece, the magnetic field configuration of Figure 14 was obtained. The performance data obtained with such a field and with the 5-cm diameter shield in place(shields are discussed in a later section) are presented in Figure 15. These data show a general decrease in performance with increasing cathode field.

By examination of Figures 10 and 14, it is evident that when the cathode magnetic field opposes the main field, the resulting field lines tend to diverge just upstream of the baffle. This divergence of field lines appears to be such as to encourage electron flow toward the annular opening between the baffle and the pole piece. The ultimate field configuration may be one where a critical field line reaches from the cathode to the baffle aperture, much as suggested in reference 5 for the main discharge. As an approach to this concept, a double solenoid configuration was tried, as described in the next section.

Double Solenoid

From inspection of Figure 10, it can be seen that the magnetic field lines that pass near the baffle aperture do not originate near the cathode. Displacement of these field lines inwards to be near the cathode could be accomplished by the addition of another solenoid coil as shown in Figure 16(a).

Typical magnetic field configurations with the secondary coil are shown in Figure 16(b) shows the magnetic field shape when the secondary coil is aiding the main field, and when the single-solenoid coil is opposing the main field.

The magnetic configuration shown in Figure 16(b) approaches most nearly the intent of forming a critical field line reaching from the cathode to the baffle aperture. Coil currents used in obtaining the patterns shown in Figures 16(b) and (c) were greater than those used in thruster operation. From inspection of the field pattern shown in Figure 16(b), it can be surmised that the thruster data was taken at less-than-optimum field strengths.

The results obtained with this coil are shown in Figure 17, where it is evident that the performance is improved by increasing the secondary-coil magnetic field strength. However, as shown in Figures 17(a) and 17(b), the mere presence of the secondary coil tends to increase the discharge power. This degradation of performance by the presence of the secondary coil might be avoided by the use of a conical shield, which is discussed in a later section. The most pronounced effect was the impossibility of running the thruster when the cathode pole piece field was opposing the primary cathode field. As illustrated in Figure 16(c), such a configuration tends toward restriction of electron flow from the cathode.

Simple Solenoid with Baffle Solenoid

A coil was placed on the main-discharge side of the baffle in an attempt to shape the field lines in the baffle aperture thereby reducing electron impingement on the baffle. The design of the baffle coil is shown in Figure 18.

Figure 19 summarizes the effect of the baffle coil. Data are presented for one main and primary pole piece field condition and various baffle secondary coil field conditions. Here, too, the increased surface area exposed to the main discharge causes a degradation that exceeds any anticipated improvement. In addition, the coil may not have been sufficiently large to deflect electrons away from the coil to the extent anticipated. For this experiment, there are discrepancies in the sets of data presented. In Figure 19(a), it seems that the baffle coil had a positive effect in reducing discharge losses, while in Figure 19(b), the baffle coil seems not to have any effect at all. The causes of these discrepancies are not known at the present time.

SHIELDS

by G. Palumbo, R. Vahrenkamp, and D. Fitzgerald*

Attempts to improve performance by variations of the pole piece geometry were mainly focused on decreasing the volume of the discharge region by adding shields of different diameters and shapes so as to decrease the area exposed to the cathode region ion flux.

Cylindrical Shields

The pole piece volume was varied by inserting stainless steel shields of various diameters in the manner illustrated in Figure 20. The baffles used with each shield were selected so the ratio of open-area to colsed-area between the cathode and main discharge region was roughly constant. All baffles and shields were allowed to float.

In Figure 21, data taken with the cylindrical shields are summarized. They suggest that a reduction of surface area in the discharge region of the pole piece does reduce the discharge losses by reducing ion flux to the walls up to a point. Further reduction in surface area by reducing the shield is ineffective.

5-cm diameter shields. The combined effect of both the 5-cm diameter shield and a cathode field is illustrated in Figure 22. This figure shows a decrease in discharge losses with increasing cathode field, but the improvements are not as significant as when the cathode pole piece works alone. This effect is better visualized in Figure 23 in which the effect of cathode field at 90% utilization on the performance is summarized. It indicated there is an optimum cathode field

---

*Graduate Research Assistant, doctoral student

for each main discharge field. This is confirmed in Figure 24, where the effects of field on arc voltage and beam current are reported. The arc voltage and beam current are both increased by about 4%; in comparison, the configuration without shield (Figures 9 and 13) had an increase of about 6.5% of both arc voltage and beam current when the cathode field was applied. This difference might be due to experimental error, although the consistency of the data suggests there may be an actual trend. Baffle open areas with various configurations are listed in Table I. Presence of the coil in the single-solenoid configuration may have been responsible for a reduction in the open area shown in Table I, but it can be concluded that the open area is considerably less for the 5-cm shield configuration, which implies a greater impedence between the cathode discharge and the main discharge for that configuration. This is borne out by comparison of Figures 13 and 24 which shows that the 5-cm shield configuration has a higher base (zero cathode coil current) discharge voltage. However, the presence of the 5-cm diameter shield in the baffle open-area region may be interfering with the magnetic field configuration (see Figure 10) as indicated by the data in Figure 25 which is discussed below. If this reasoning is correct, then greater changes in beam current and arc voltage should be expected for the single-solenoid configuration with no shield. Definite reasons for these trends can be established only with additional data.

Small cylindrical shield. The effects of the smaller shield (3.5-cm diameter) are given in Figure 25 and it is evident that with this configuration the effect of the coil on performance is reversed, since the ev/ion increases with increasing cathode-pole-piece field. As discussed above, it is believed that the presence of shields near the baffle open area may interfere with the magnetic field inside the pole piece

thereby increasing the discharge power. Future experiments with shortened shields may bear out this explanation.

Conical Shield

The last attempt to change the pole piece geometry was made by using a conical shield as in Figure 26. This shield seems to reduce the discharge losses at high mass utilization as is apparent in Figure 27. In this figure, three cases are compared; the 5-cm diameter cylindrical shield with and without a secondary coil, and the conical shield, all with no cathode field applied. From this graph it appears that the conical shield is slightly more effective than the cylindrical shield at high utilization.

The effects of floating surfaces and grounded surfaces in the cathode pole piece region, are compared in Figure 28. These data were obtained with the conical shield grounded and floating, and they indicate a slight improvement in performance when the shield is floating.

The effect of both conical shield and cathode-pole-piece field are shown in Figure 29 for the case of this shield at cathode potential and in Figure 30 for the shield at floating potential. These figures show that slight improvements in performance can be achieved by applying a magnetic field in the cathode discharge region with shields present.

Al illustrated in Figure 31, the difference in performance due to holding at cathode potential or floating the shield is minor. Comparison of these data with those of Figure 27 shows the conical and cylindrical shields are equally effective in improving performance.

PLASMA FLUCTUATIONS

by D. Fitzgerald

An x-y oscilloscope was installed in the facility several months ago to monitor the voltage and current characteristics of the arc, magnet, and keeper power supplies in order to ascertain the amount of ripple present during thruster operation. The oscilloscope was also used to observe the voltage-current characteristics of a Langmuir probe and the voltage response of a floating emissive probe positioned within the thruster. The following observations are for the present mostly qualitative for reasons which will be given below.

The power supplies under scrutiny mentioned above were tested beforehand with purely resistive loads. The resistors were chosen such that the load would be comparable to the maximum power requirements which might be met during thruster operation. The amount of ripple present under maximum current conditions was not considered unreasonable (about 10% for the magnet and keeper, and less than 5% for the arc supply).

The same parameters taken under actual thruster operating conditions were found to be characterized by the presence of high frequency disturbances (on the order of 20 kc). All three power supplies showed current fluctuation amplitudes that were considerably larger (on the order of the DC current signal itself) than the keeper current disturbance.

The thruster was normally run with the magnet current at about 1.7 amperes where the observed frequency was approximately 20 kc. The frequency of the disturbance increases in nearly a linear fashion with increases in magnet current over a range from about 0.5 to 2.5 amperes (where the discharge becomes highly unstable). The disturbance appears to change mode and couple to a lower frequency (pulsing) signal at less than 0.5 amperes magnet current. The amplitude of all these fluctuations appear to be dependent on the level of arc current and to a lesser extent

on the magnet current. The amplitude and frequency are reduced by a factor of two when the beam is not being extracted. These observations were made during experiments directed at other areas; therefore, there was neither time nor the proper facilities to completely explore this phenomena. Many changes were made on the power-supply filters in an attempt to remove these fluctuations. These changes benefited the keeper power supply but had little effect on the magnitude and frequency of the magnet and arc current fluctuations. The lack of any significant effect on frequency during these changes apparently rules out the likelihood of a resonance between the discharge and the power supply. The facility is presently being equipped with a regulated arc supply on loan from the Jet Propulsion Laboratory. This change will hopefully settle the question of power supply resonance.

A Langmuir probe placed within the thruster was swept with a saw tooth waveform with respect to cathode potential. The waveform was +60 volts maximum at a frequency of about 2 kc. The current-voltage characteristics were displayed on the x-y oscilloscope utilizing a 10 ohm shunt resistor to measure the probe current drawn. The resulting display indicated the presence of oscillations similar to those found by previous workers (Figure 9 of reference 6).

A floating emissive probe, similar to the one described in reference 7, was placed in the same position as the Langmuir probe. The current to the emissive probe heater was increased up to a point where the floating probe potential (with respect to cathode) did not change significantly with further increases in heater current. When this condition was met, the probe was assumed to be at or near the local plasma potential. The mean value of the plasma potential was about the same as the arc voltage (30 volts) and it demonstrated characteristics almost identical to the arc voltage in the magnitude (about 5 volts) and frequency of the fluctuations present. The size of the noise envelope on the Langmuir probe characteristics mentioned

above is in line with this 5 volt figure; therefore, it may be substantially eliminated by referencing the Langmuir probe sweep to the local plasma potential. Assuming the addition of the regulated arc supply does not eliminate these fluctuations, the following future experiments are suggested from the observations mentioned above.

(A) The plasma potential throughout the thruster will be compared to the arc voltage to determine whether correlations exist in the wave shape and phase. This experiment would necessitate the use of a dual trace oscilloscope and a movable emissive probe.

(B) A Langmuir probe will be swept with respect to the local plasma potential by means of an emissive probe in close proximity to the Langmuir probe. This requires the use of an emitter-follower amplifier in conjunction with the emissive probe to establish the plasma potential reference.

(C) The frequency power spectrum of the disturbance should be measured as a function of thruster parameters and the relationship between the power spectrum and thruster performance should be established.

(D) Similarities between these phenomena and other observations commonly referred to as plasma turbulence. should be explored. In particular, innovations which have succeeded in reducing the turbulence should be attempted. For example, certain types of instabilities have been suppressed by the addition of a quadrupole magnetic field applied transverse to the axial magnetic field in a Penning discharge (reference 8). A quadrupole magnetic field also has been applied to a mercury bombardment thruster (reference 9), and was found to attenuate the fluctuations.

CONCLUDING DISCUSSION

It has been pointed out that a conical baffle or the use of a field coil on the outside of a flat baffle results in a degradation in performance. It appears this occurs because of the increase of surface area exposed to the discharge on which ions can recombine. The coil had the further disadvantage of being at cathode potential and it therefore distorted the electric field lines within the main discharge region.

Shields installed within the cathode pole piece have been shown to be an effective means of improving performance. Improvements of about 30 ev/ion at 90% utilization have been achieved apparently because of the reduction in surface area within the cathode discharge region. The shape of the shield (conical or cylindrical) seems to have minor effect on performance, and floating shields tend to produce very slight improvements above the case of shields held at cathode potential. Very small diameter shields produce increases in discharge losses. It is possible that this degradation of performance occurs because of the opposing effects of reduced surface area inside the pole piece, and of increased ion density. As shield diameter is decreased, the surface area decreases in proportion to diameter d. However, the flow cross-sectional area decreases in proportion to d^2, hence ion density increases faster than surface area is decreased.

Significant improvements in performance (about 20 ev/ion at 90% utilization) have been observed when an axial magnetic field is applied within the cathode discharge region. This is probably due to increases in electron densities and electron energies in the main discharge region. These effects were discussed in reference 2. There are two possible reasons why the field is most effective when it is opposing the main field. The field aids in extraction of electrons from the pole-piece region into the main discharge thereby increasing the number of primary electrons in the main chamber. Such increase in primary electrons will result in a higher ionization probability (and higher ion density), and therefore a larger beam current.

The other effect that is evident is an increase of discharge voltage and therefore higher energy primary electrons. These effects reach an optimum beyond which the cathode pole-piece field is ineffective.

Reductions in shield area have the tendency to decrease the discharge losses to a point, beyond which further reduction is ineffective or even deleterious. A possible explanation of this area effect is that the reduction of area exposed to the discharge reduces the ion flux to the walls. As the shield diameter is decreased, however, the cross-sectional area for propellant flow is also reduced, thereby increasing the ion density. The overall effect is one where very small shield diameters may cause excessively high ion densities, with a net increase in ion loss to the walls.

The second possible explanation could be the comparison between the solid angle for electron escape to the main discharge, and the area effect. As long as the area reduction does not greatly affect the solid angle, increases in performance will result. A further reduction of area will reduce the solid angle to a point where the electron path will be greatly affected, and a decrease in performance will result.

The effect of combination of shield and single-solenoid could be explained by considering the arc voltage and beam current. The performance increases as beam current is increased at the same arc power. The beam current can be increased by an increase in ionization in the chamber and ionization is effected by the number of primary electrons and the energy given to them.

It has been pointed out previously that a single-solenoid magnetic field has the tendency to increase the arc voltage and therefore increase the energy given to the electrons. Also, reduction of wall area by use of shields has a tendency to increase the arc voltage. However, these trends are not additive; perhaps because large reductions in shield diameter require much greater magnetic field strengths inside the pole piece region for the same improvement in electron extraction. From the data obtained so far, the effect of a secondary coil is not clear. Further data should be taken over a wider range of magnetic field strengths, and supported with field-pattern measurements.

REFERENCES

1. Fitzgerald, D., and Vahrenkamp, R.: Performance Mapping of 20-cm Hollow Cathode Mercury Ion Thruster. Final Report, NASA Grant NGR06-002-032, Advanced Electric Propulsion Research. May, 1969.

2. Masek, T.D.: Plasma Properties and Performances of Mercury Ion Thruster. AIAA Paper No. 69-256, AIAA 7th Electric Propulsion Conference, Williamsburg, Virginia. March 3-5, 1969.

3. Palumbo, G., Wilbur, P., and Vahrenkamp, R.: Experimental Investigations into the Performance of a 20-cm Hollow Cathode Thruster. Annual Report, NASA Grant NGR06-002-038. September, 1968.

4. Poeschel, R.L., and Knauer, W.: A Variable Magnetic Baffle for Hollow-Cathode Thrusters. AIAA Paper No. 70-175. January, 1970.

5. King, H.I., Poeschel, R.L., and Ward, T.W.: 2½ KW Low Specific Impulse Hollow Cathode Mercury Thruster. AIAA Paper No. 69-300. AIAA 7th Electric Propulsion Conference, Williamsburg, Virginia. March 3-5, 1969.

6. Strickfaden, W.B. and Geiler, K.L.: "Probe Measurements of the Discharge in an Operating Electron Bombardment Engine", AIAA Journal, Vol. 1, No. 8. pp. 1815-1823. August, 1963.

7. Sellen, J.M., Jr.: Investigations of Ion Beam Diagnostics. Final Report, NASA Contract NAS8-1560 (TRW Systems, Inc. Report 8603-6037-SU-000). April, 1964.

8. Thomassen, K.I.: "Turbulent Diffusion in a Penning-Type Discharge", The Physics of Fluids, Vol. 9, No. 9 pp. 1836-1842. September, 1966.

9. Cohen, A. J.: An Electron Bombardment Thruster Operated with a Cusped Magnetic Field. NASA TN D-5448. September, 1969.

TABLE I - Baffle open areas for various configurations (including baffle-support blockage).

configuration	inside diam., cm.	baffle diam., cm.	baffle open area, sq. cm.	flow area, sq. cm.
pole-piece alone	6.35	5.4	6.4	31.6
single-solenoid coil	5.6	5.08	9.0	24.7
5-cm shield	5.08	4.26	3.6	20.2
3.5-cm shield	3.5	3.1	1.8	10.2
conical shield	5.08	4.26	3.6	20.2

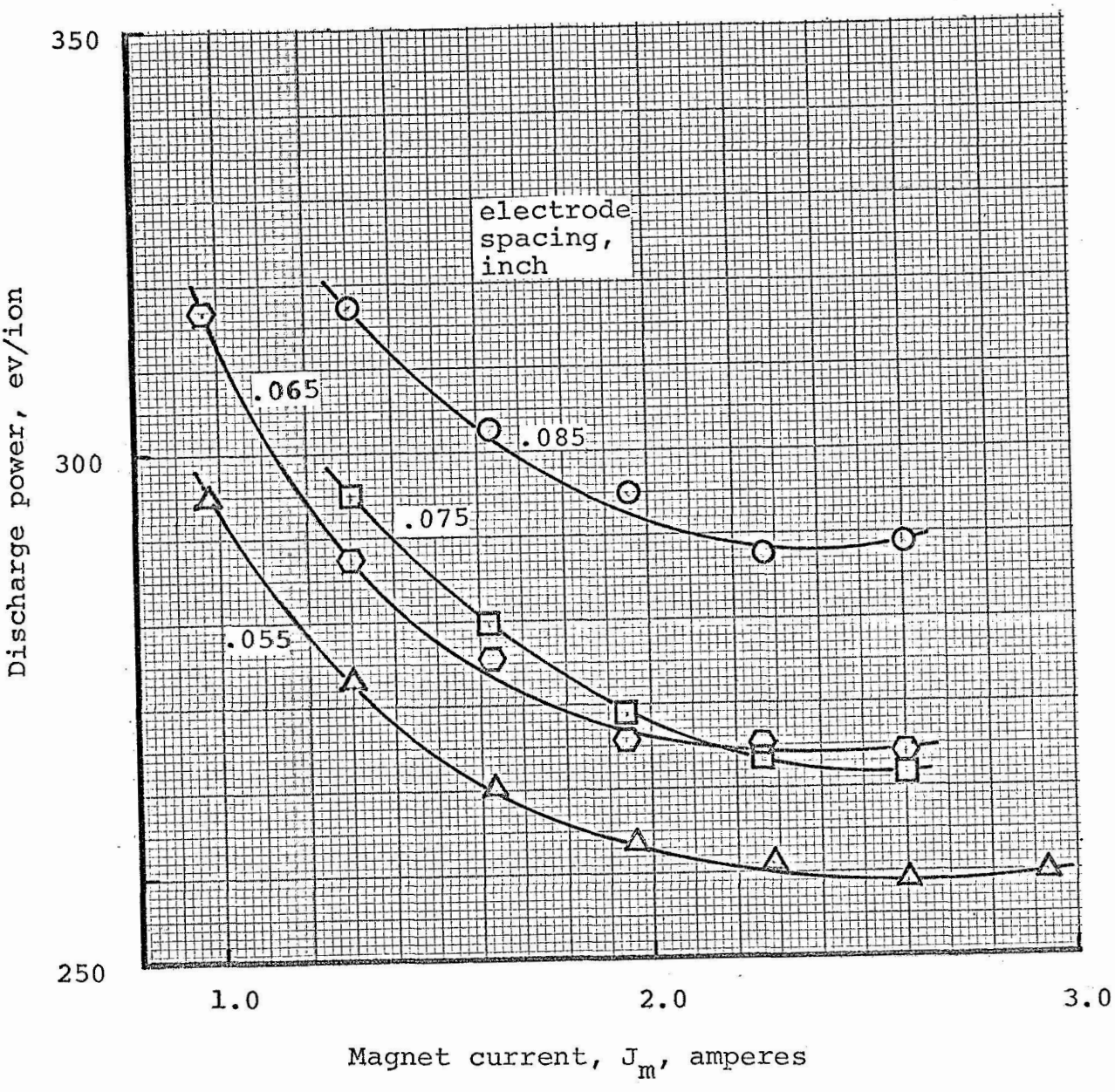

FIG. 1 - Effect of electrode spacing and magnet current on discharge power. Electrode voltages, ±2 kilovolts; utilization efficiency, 90%.

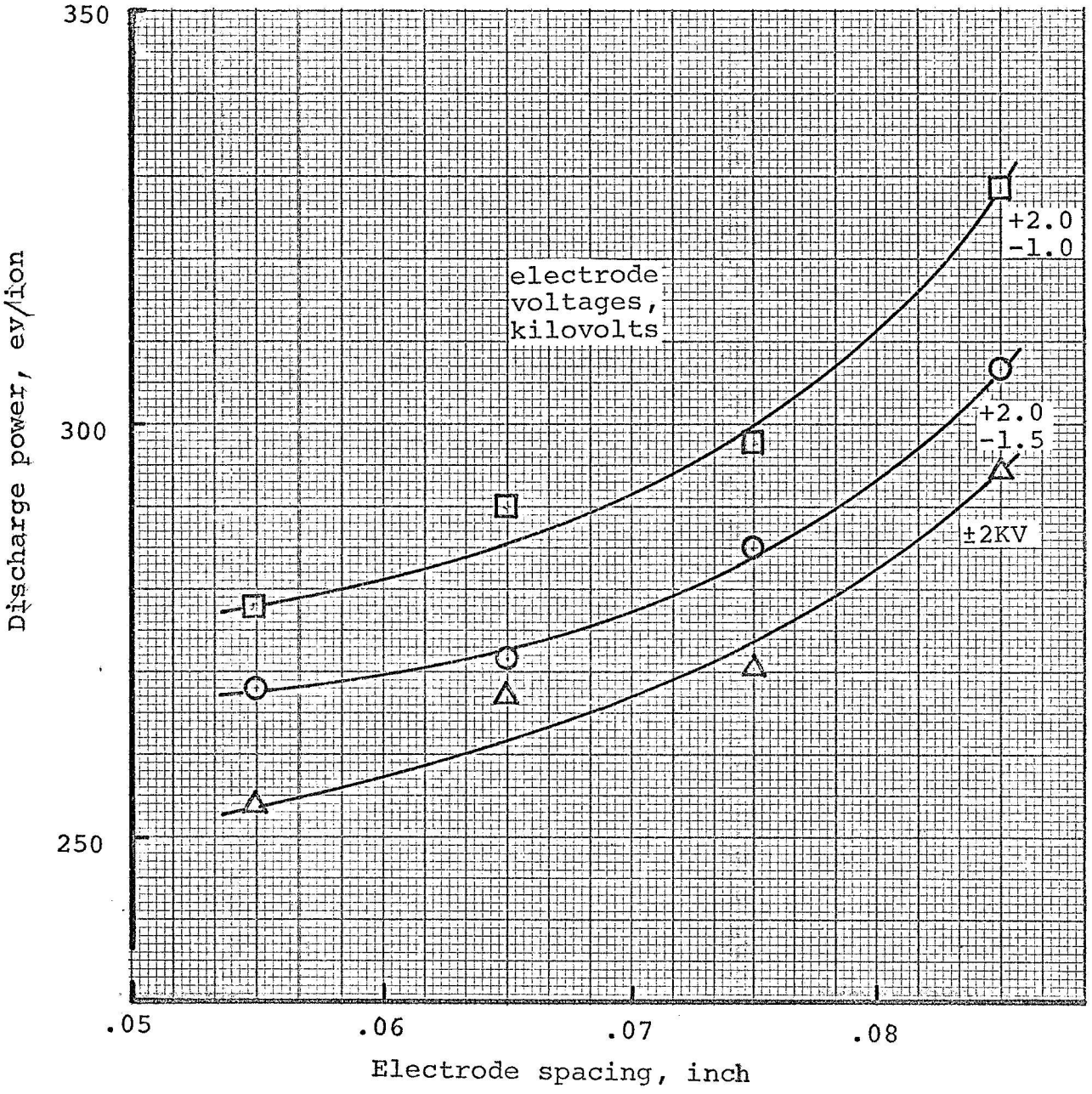

FIG. 2 - Effect of electrode spacing and electrode voltages on discharge power. Magnet current, 1.9 amperes; utilization efficiency, 90%

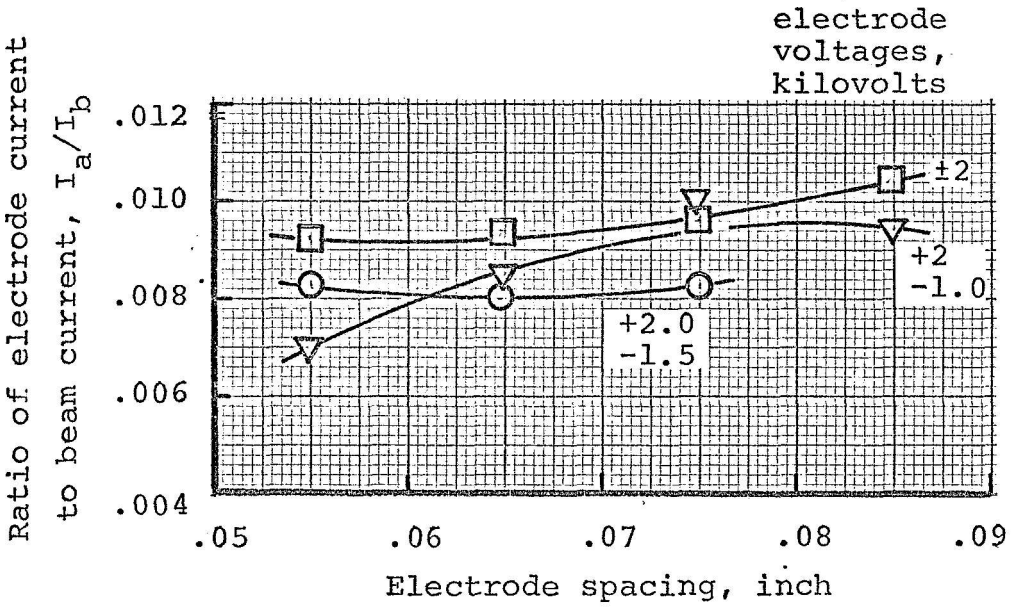

FIG. 3 - Effect of electrode spacing on accelerator impingement. Magnet current, 1.9 amperes; utilization efficiency, 90%.

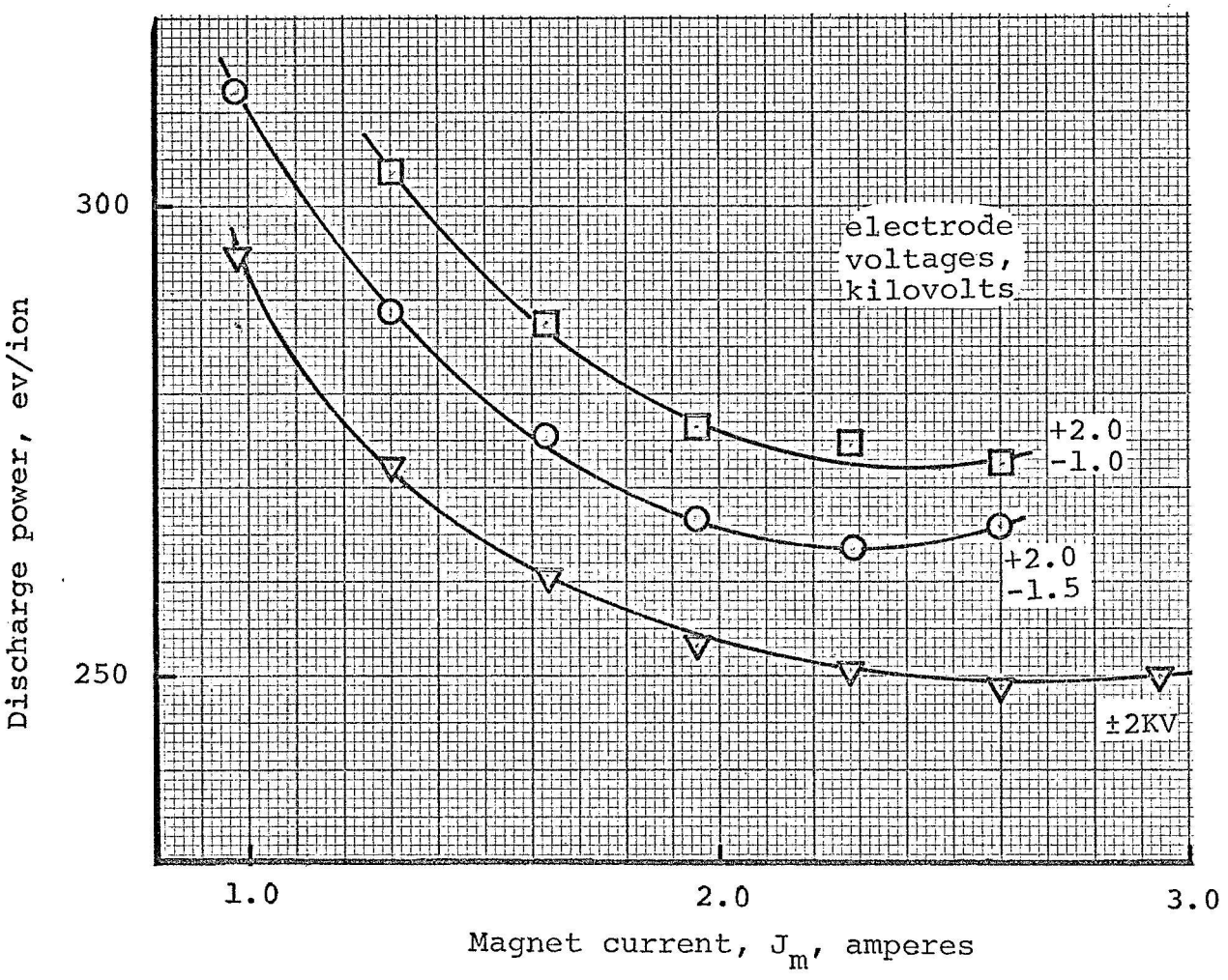

FIG. 4 - Effect of electrode voltages on discharge power. Electrode spacing, 0.055-inch; utilization efficiency, 90%.

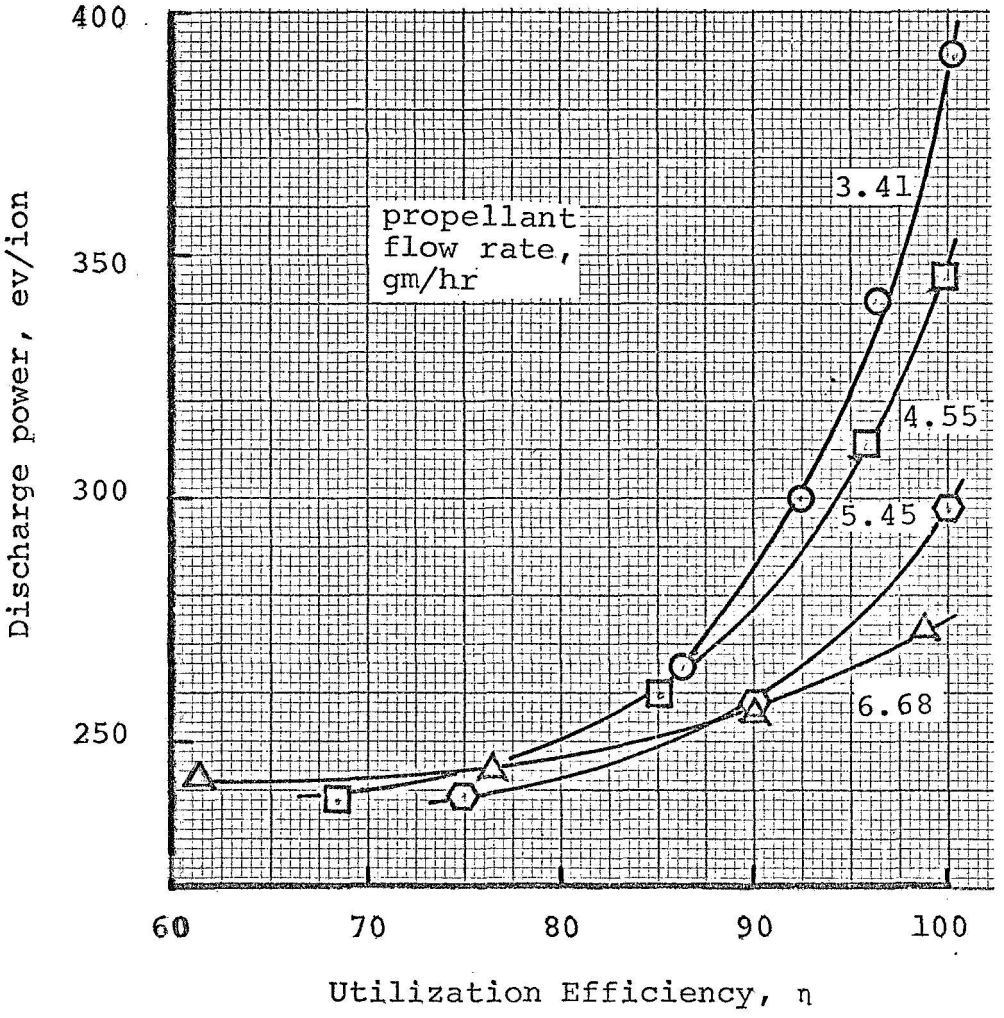

FIG. 5 - Effect of propellant flow rate on discharge power. Electrode spacing, 0.060-inch; electrode voltages, ± 2 kilovolts; magnet current, 1.9 amperes.

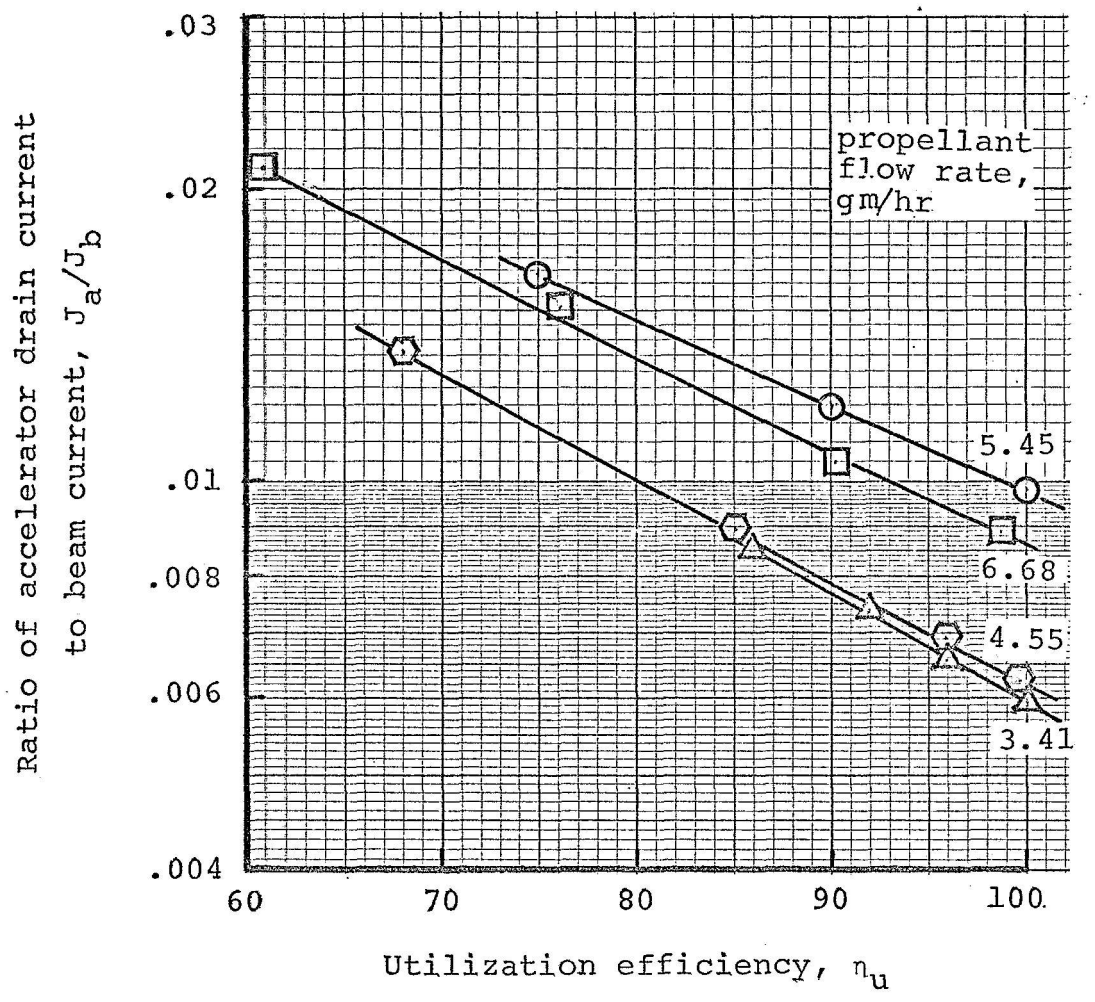

FIG. 6 - Effect of propellant flow rate on accelerator drain current. Grid spacing, 0.060-inch; electrode voltages, ± 2 kilovolts; magnet current, 1.9 amperes.

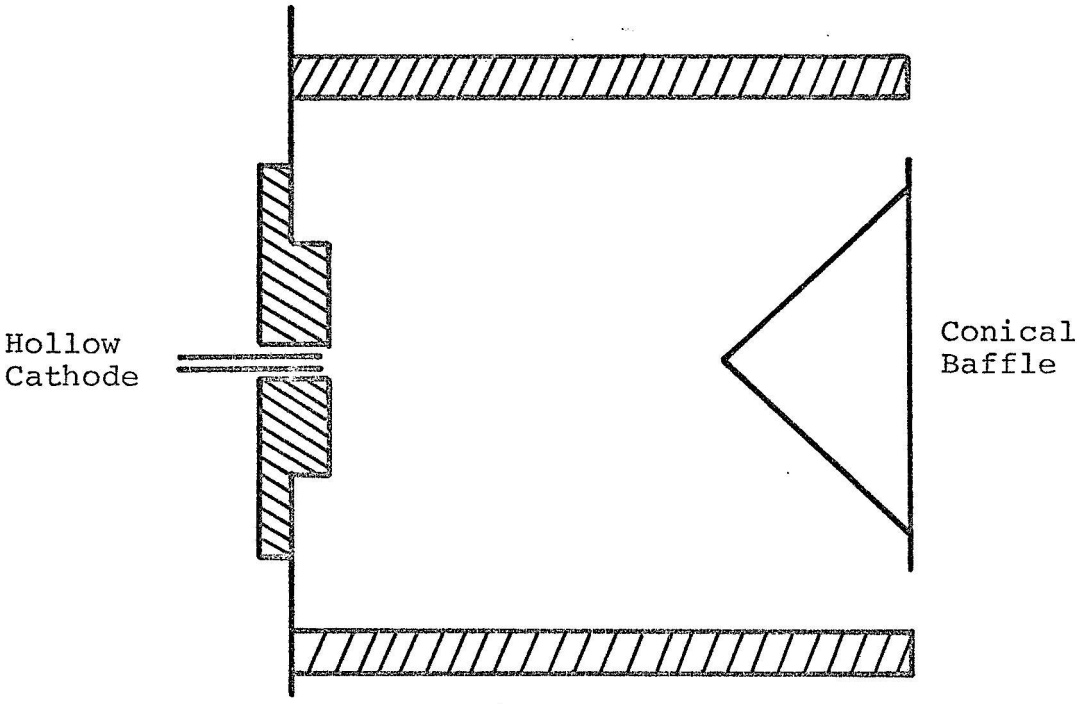

FIG. 7 - Conical baffle in cathode pole piece. Pole piece inside diameter, 6.3 cm; pole piece length, 6.3 cm; baffle diameter, 5.4 cm; baffle depth, 2.2 cm.; baffle at cathode potential.

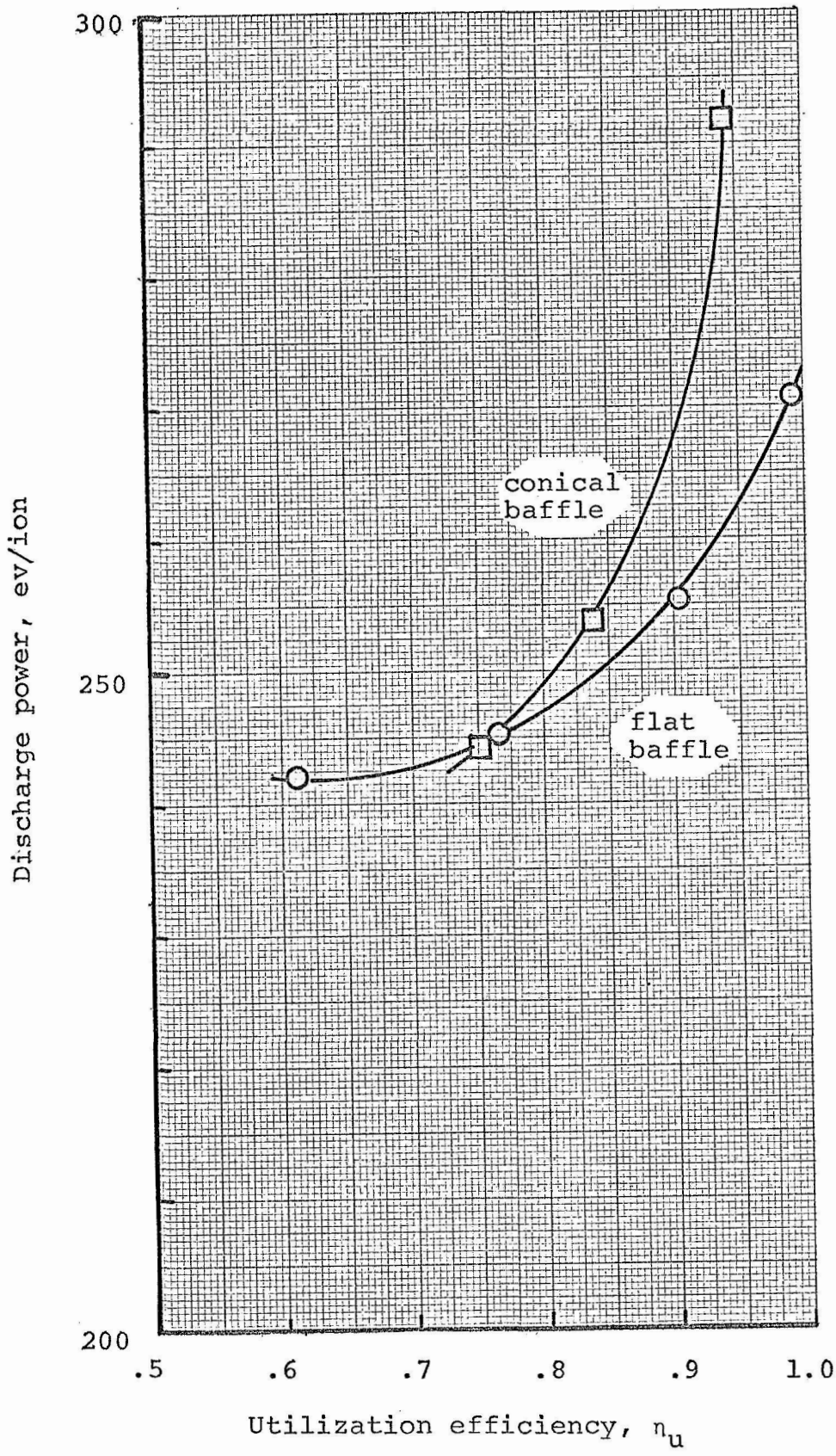

FIG. 8 - Discharge power with conical baffle. Total flow rate with flat baffle, 6.7 gm/hr; total flow rate with conical baffle, 6.4 gm/hr; magnet current, 1.9 ampere; baffle at cathode potential.

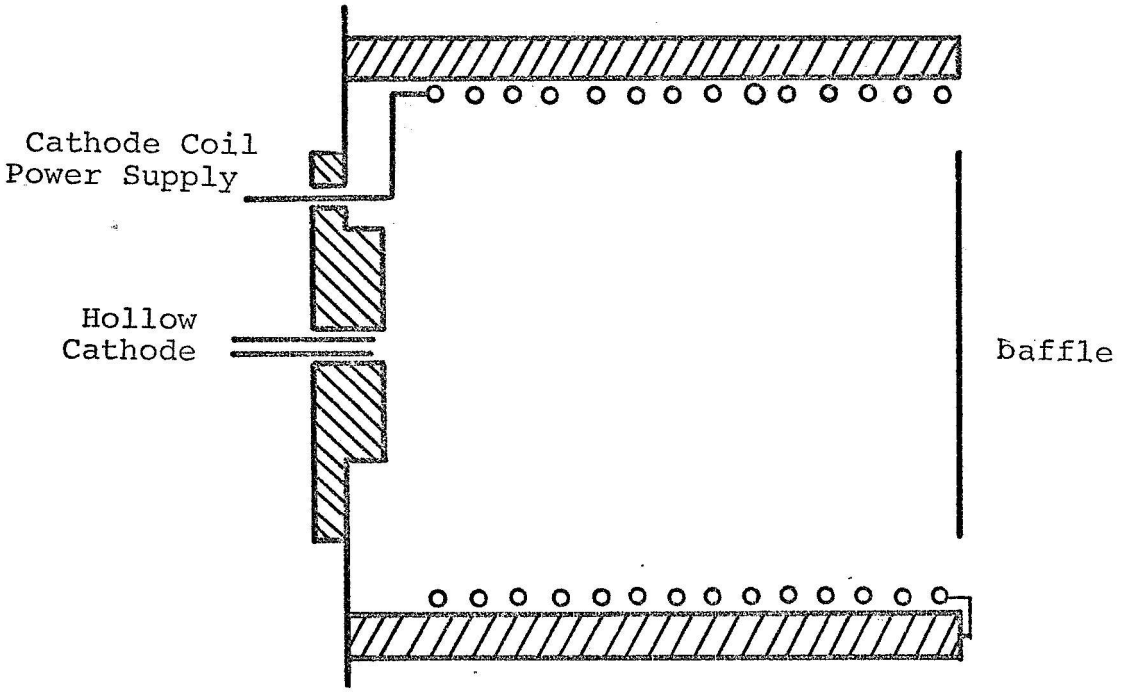

FIG. 9 - Cathode pole piece coil configuration. Coil at cathode potential, diameter 5.6 cm., length 5 cm., 420 turns/meter. Baffle, floating.

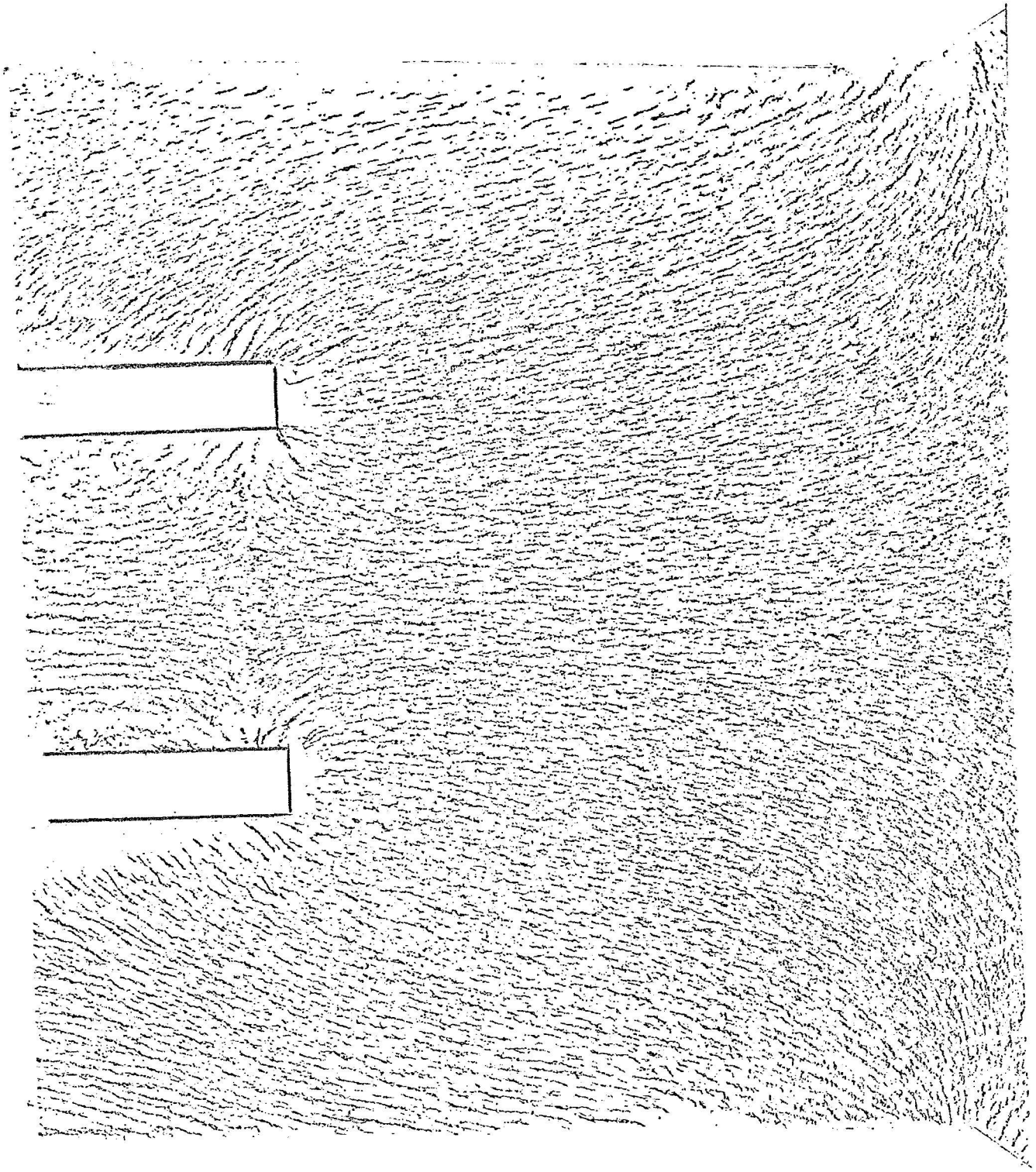

FIG. 10 - Magnetic field with single-solenoid cathode-coil opposing main field. Cathode-coil, 5 amperes; main magnet, 1.5 amperes.

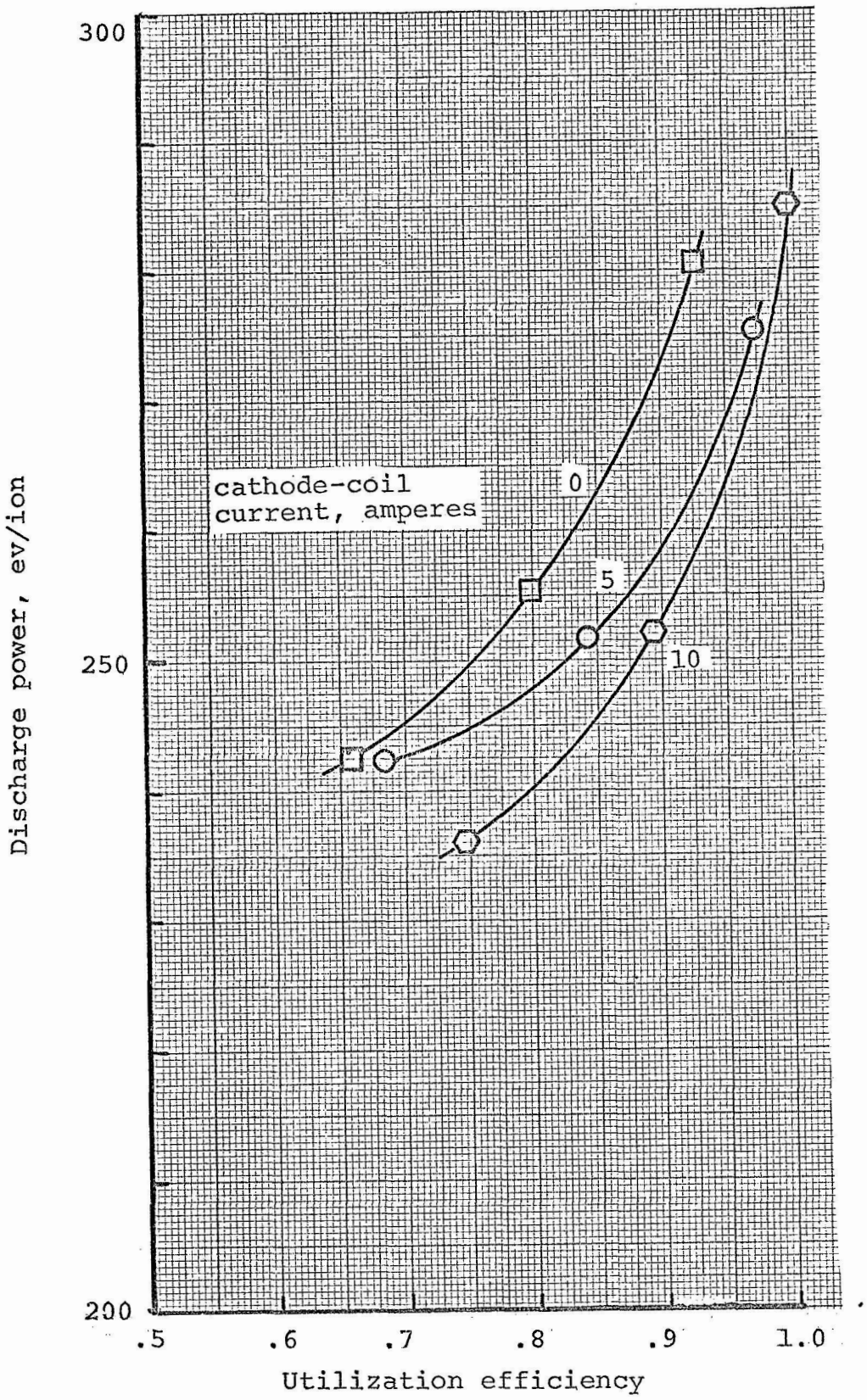

(a) main magnet current, 1.5 ampere

FIG. 11 - Discharge power with single-solenoid cathode-coil magnetic field opposing main magnetic field. Baffle floating; ratio of cathode flow to main flow, 0.12.

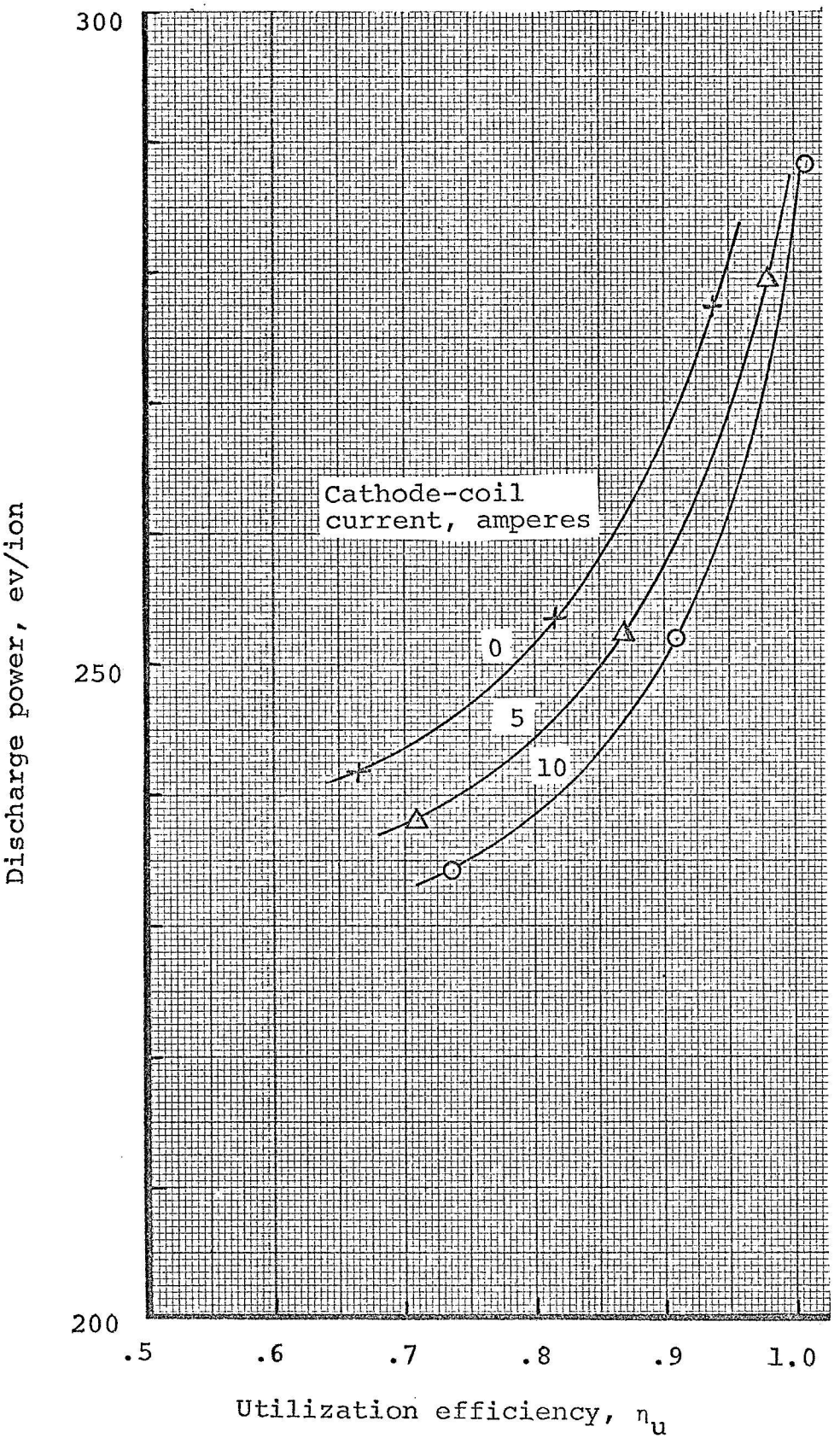

(b) main magnet current, 1.7 ampere

FIG. 11 - (cont.)

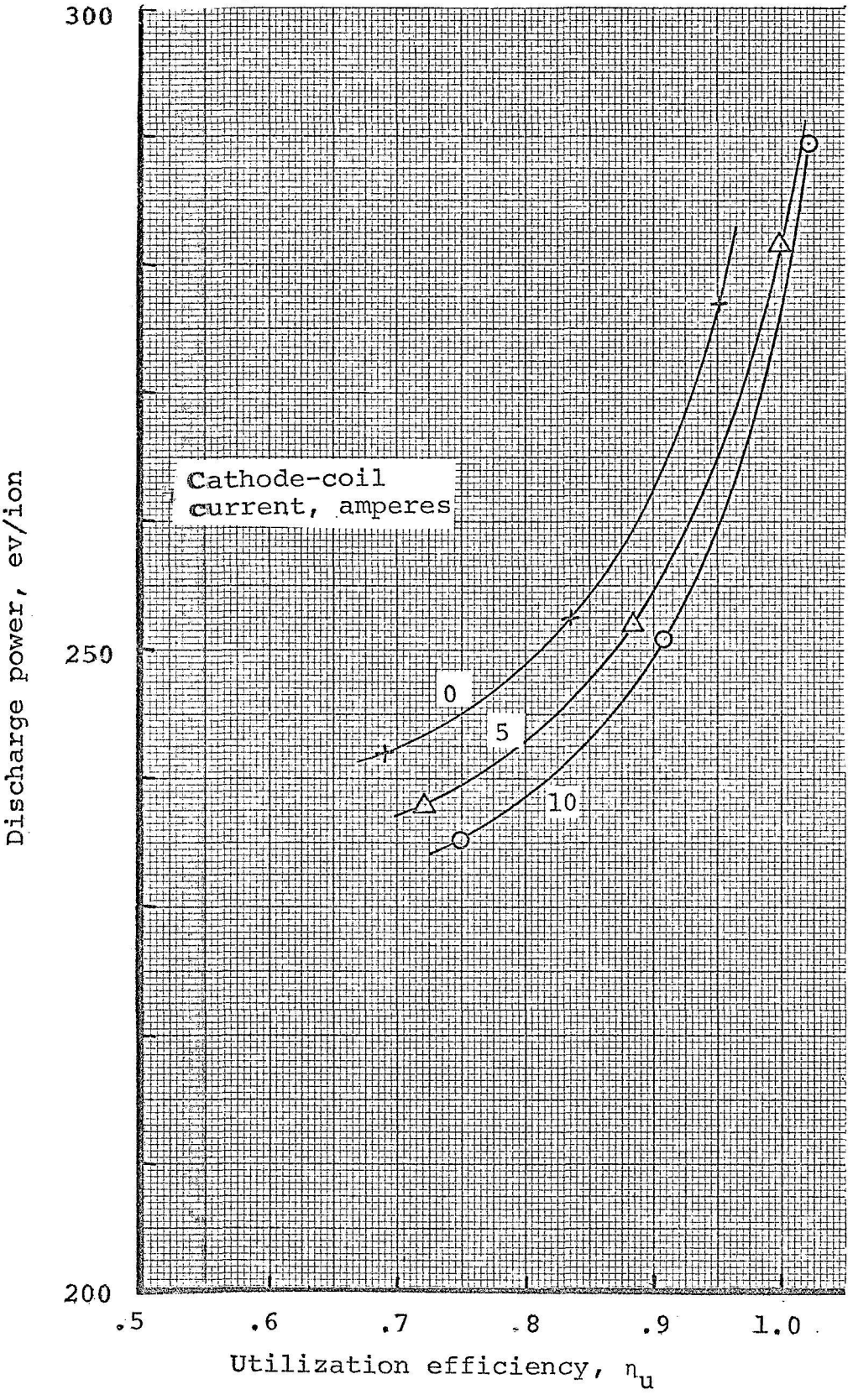

(c) main magnet current, 1.9 ampere

FIG. 11 - (cont.)

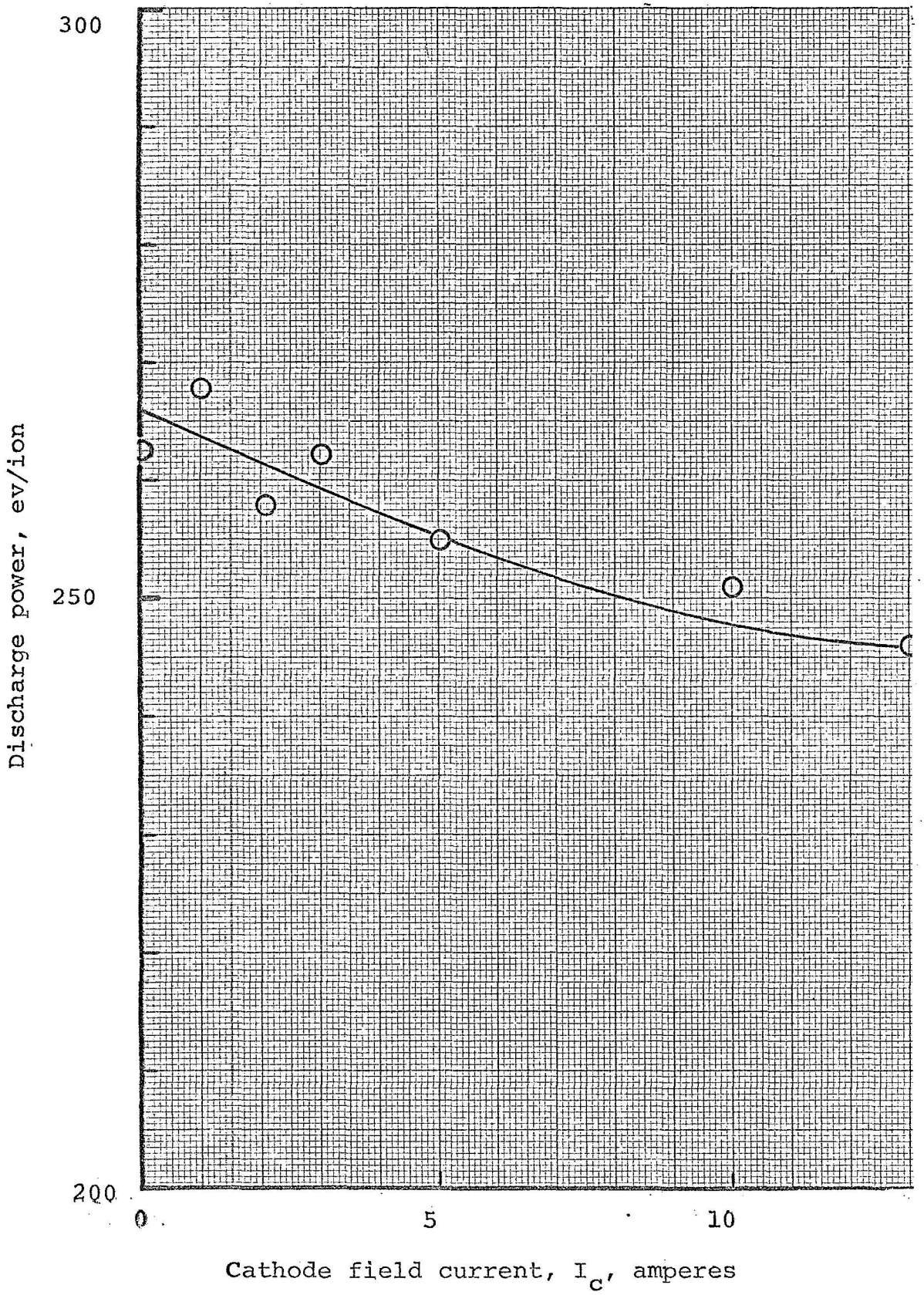

FIG. 12 - Effect of cathode field on discharge losses. Cathode field opposing; no shield; 90% mass utilization; magnet current 1.9 amperes.

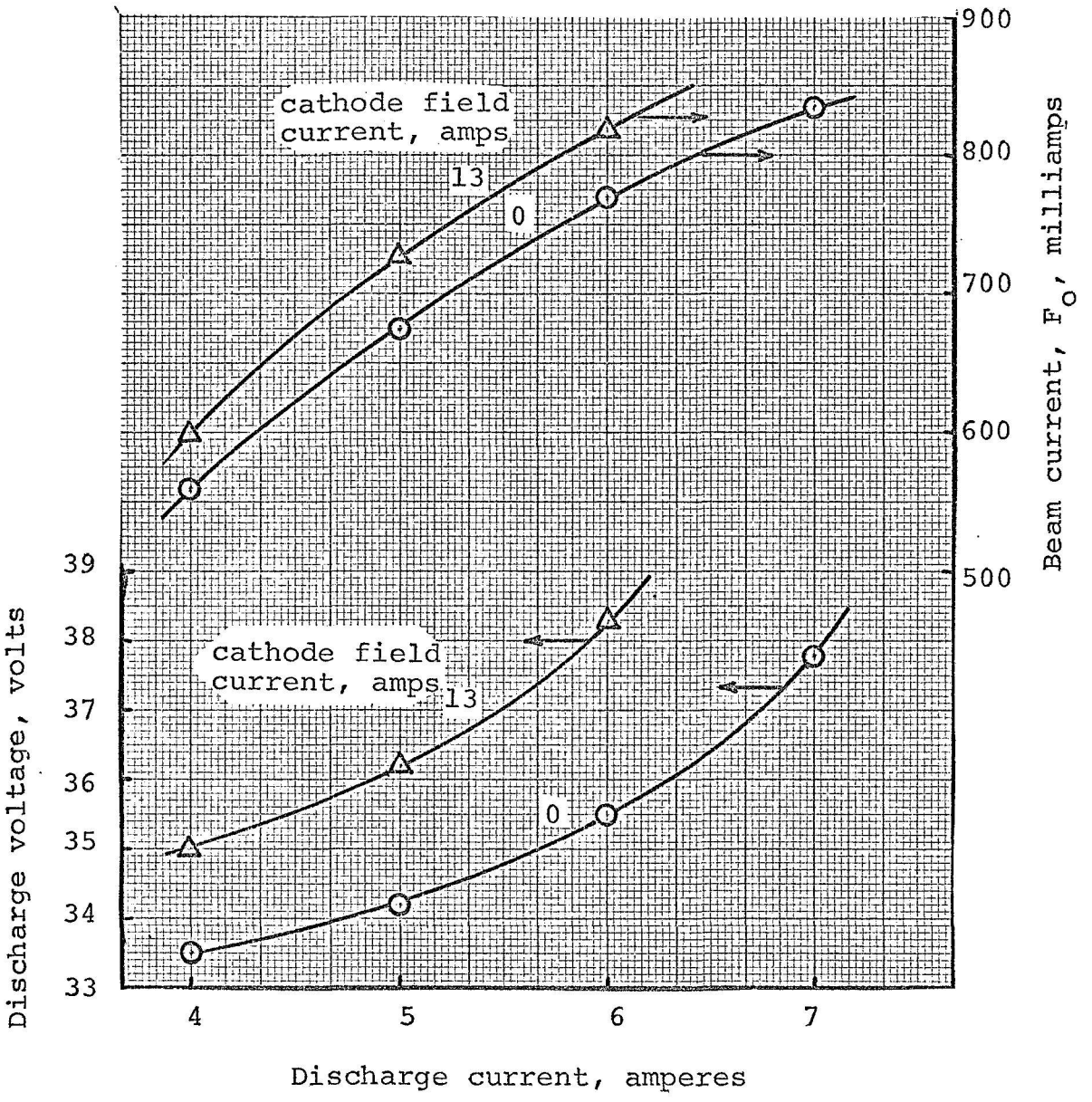

FIG. 13 - Effect of cathode field on arc voltage and beam current. Cathode field opposing main field; main magnet, current 1.9 amp; no shield.

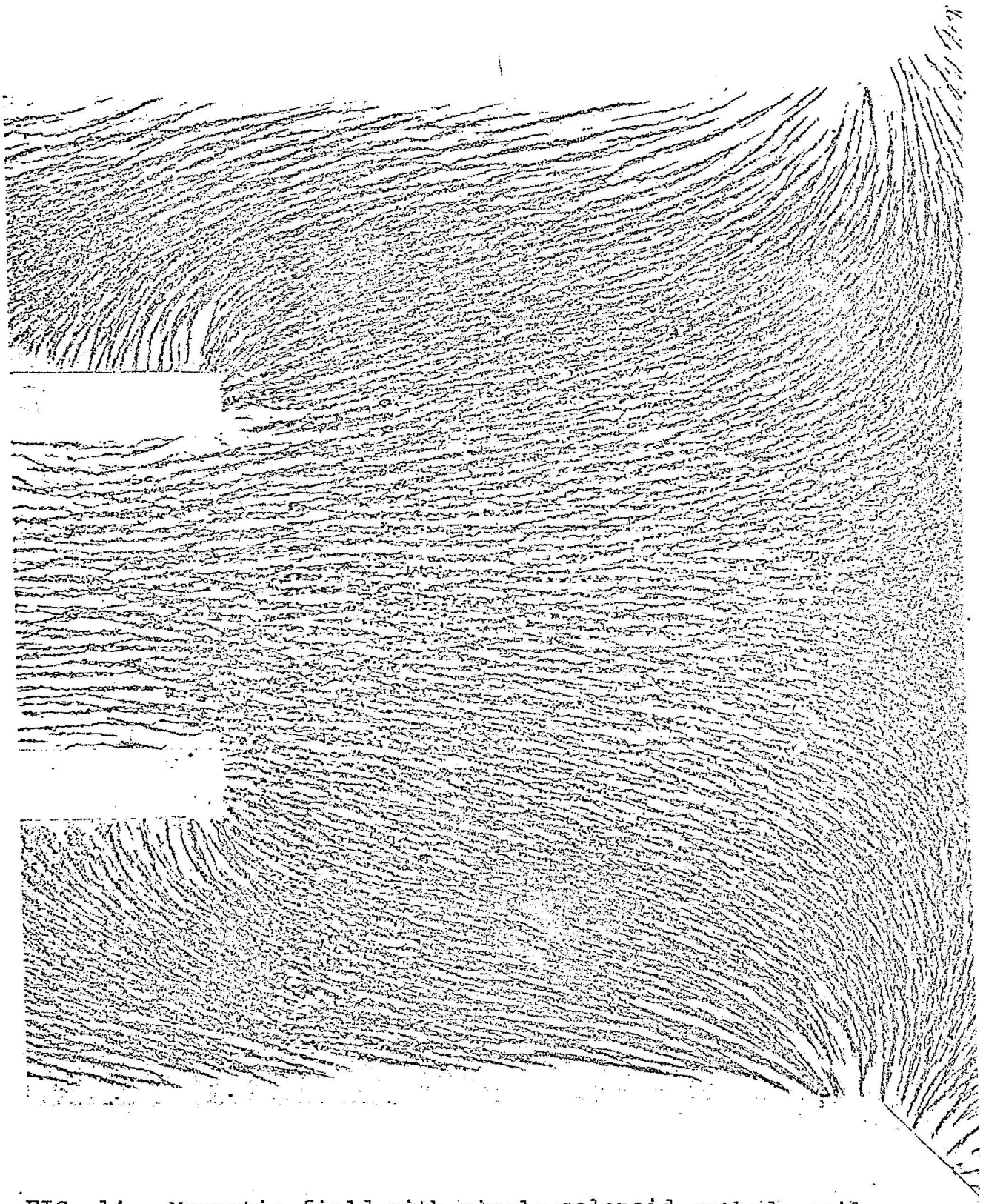

FIG. 14 - Magnetic field with single-solenoid cathode-coil aiding main field. Cathode-coil, 10 amperes; main magnet, 1.5 amperes.

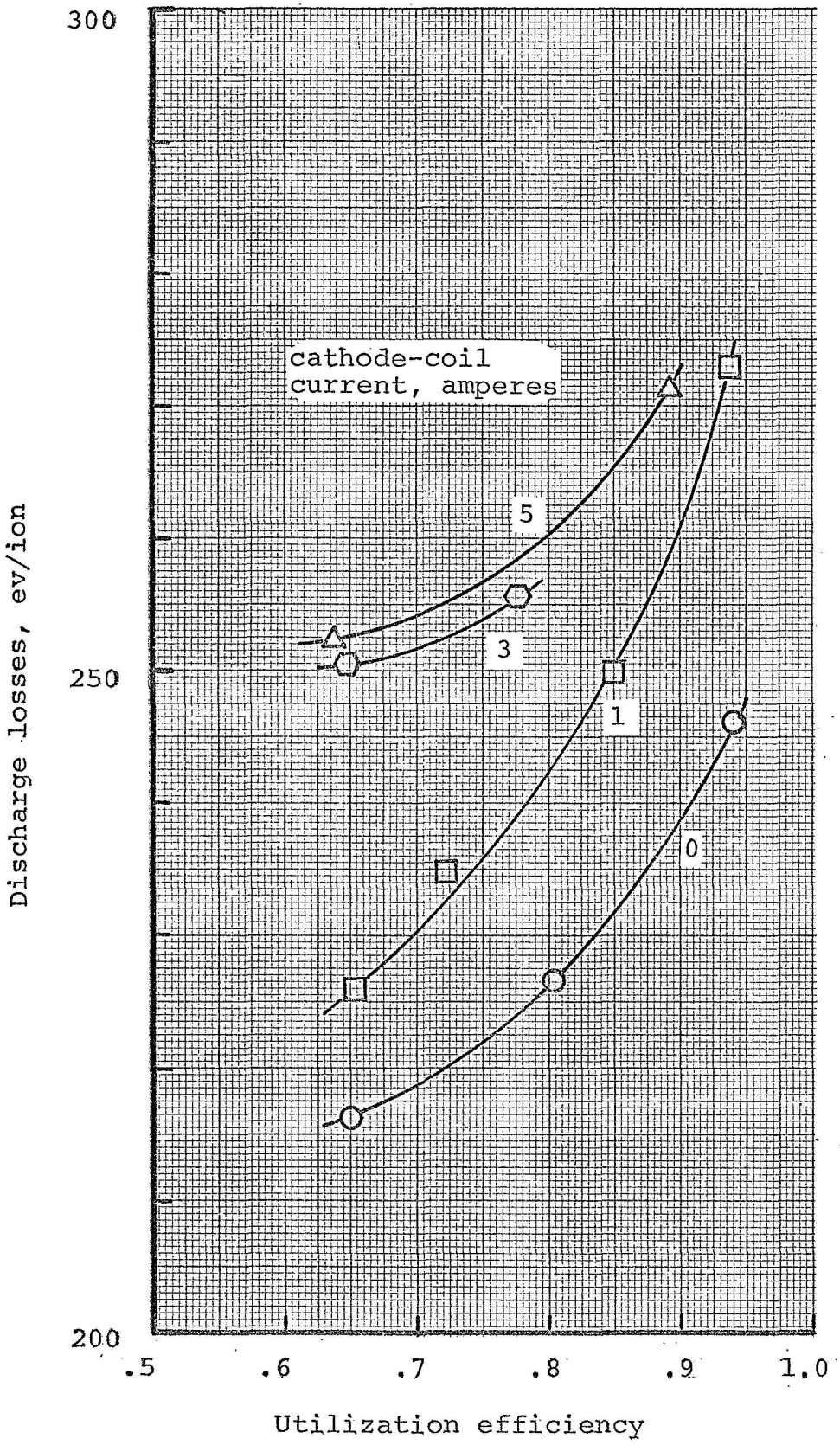

FIG. 15 - Effect of single-solenoid cathode magnetic field on discharge power with large floating cylindrical shield, and floating baffle. Total flow rate, 5.7 gm/hr; main magnet current, 1.9 amps.

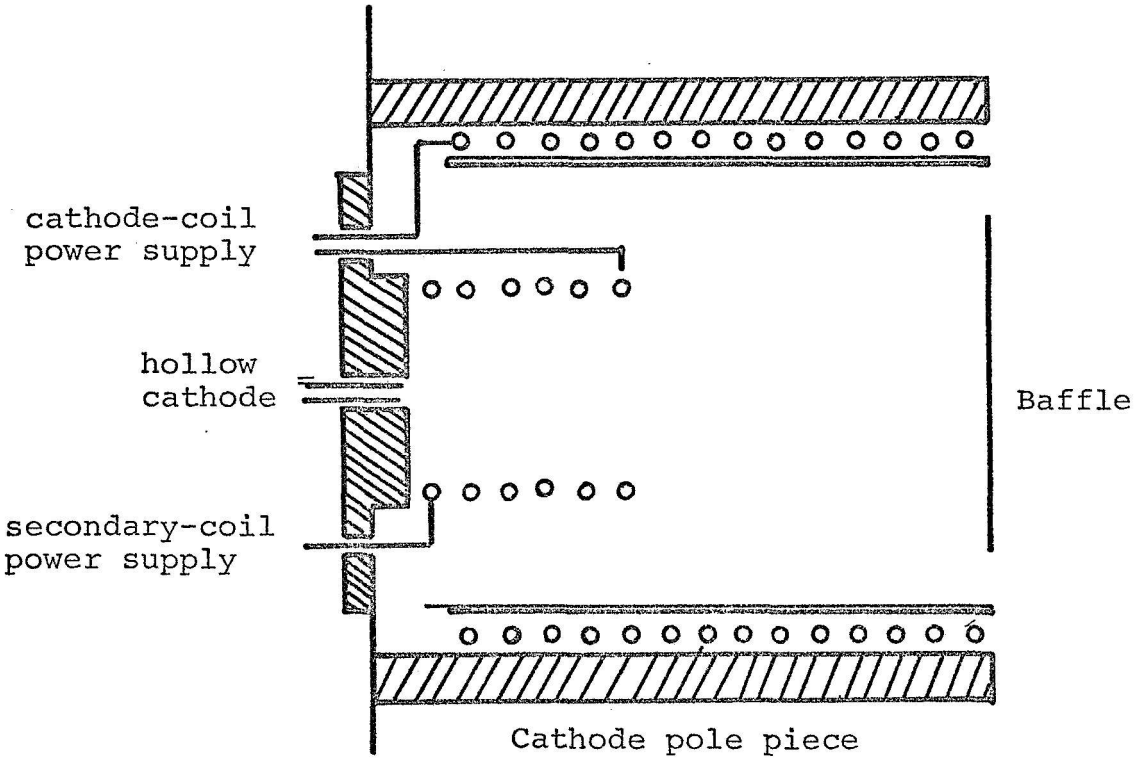

(a) secondary coil

FIG. 16 - Secondary coil and magnetic field configurations. Diameter, 1 cm., length 2.5 cm., 480 turns/meter. Coil at floating potential.

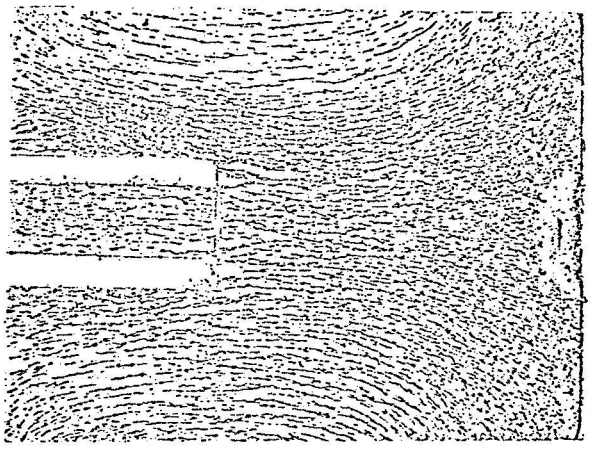

(b) secondary coil aiding single-solenoid coil, both opposing main field; secondary coil current, 30 amperes; single-solenoid coil current, 10 amperes.

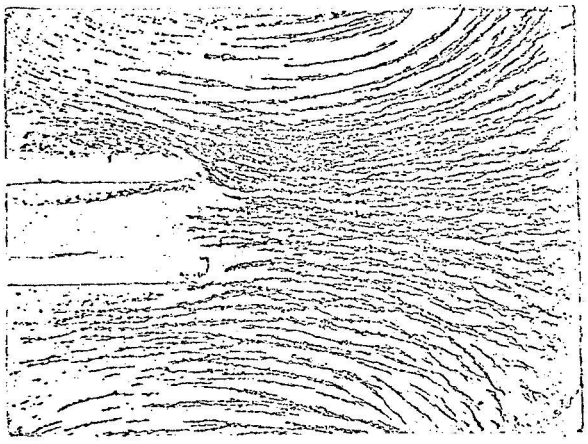

(c) secondary coil opposing single-solenoid coil, single-coil opposing main field; secondary coil current, 30 amperes; single-solenoid coil current, 10 amperes.

FIG. 16 - (cont.)

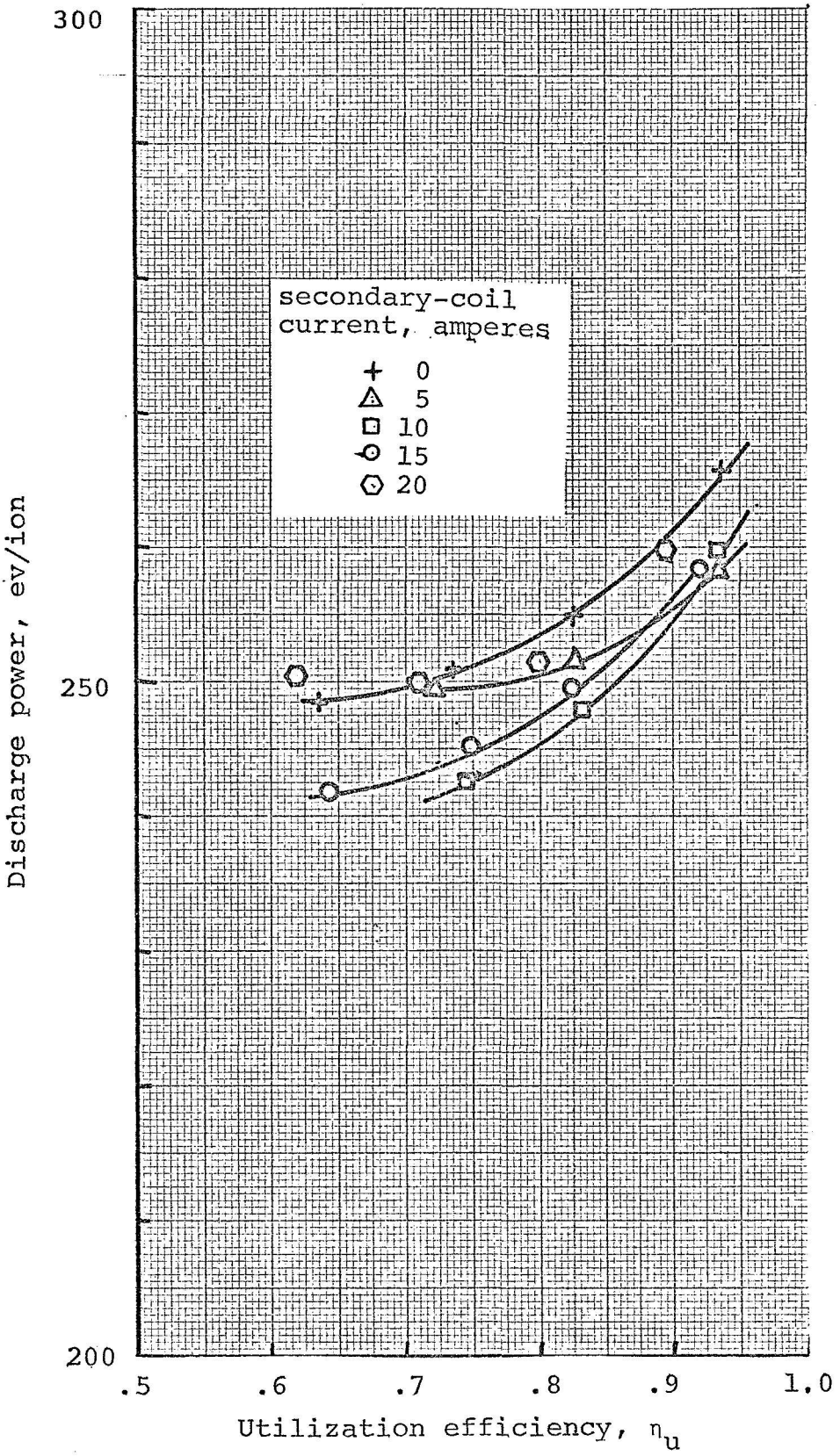

FIG. 17 - Effect of secondary coil and field in the cathode region. Main magnet current, 1.7 amperes; total propellant flow rate, 5.5 gm/hr.

(a) secondary coil current normal direction, single-solenoid coil current, 0 amperes.

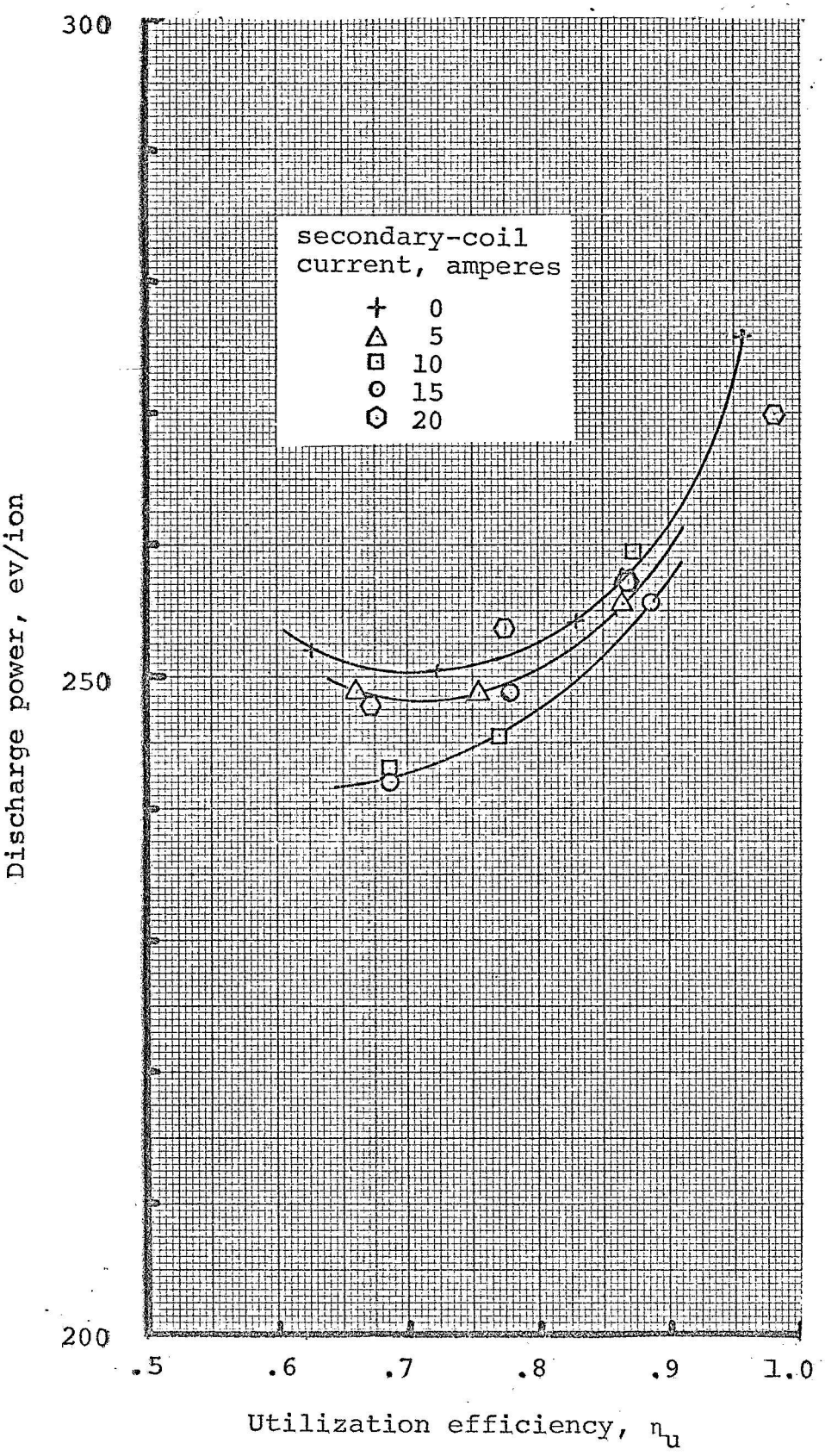

FIG. 17 - (cont.)

(b) secondary coil current reversed direction, single-solenoid coil current, 0 amperes.

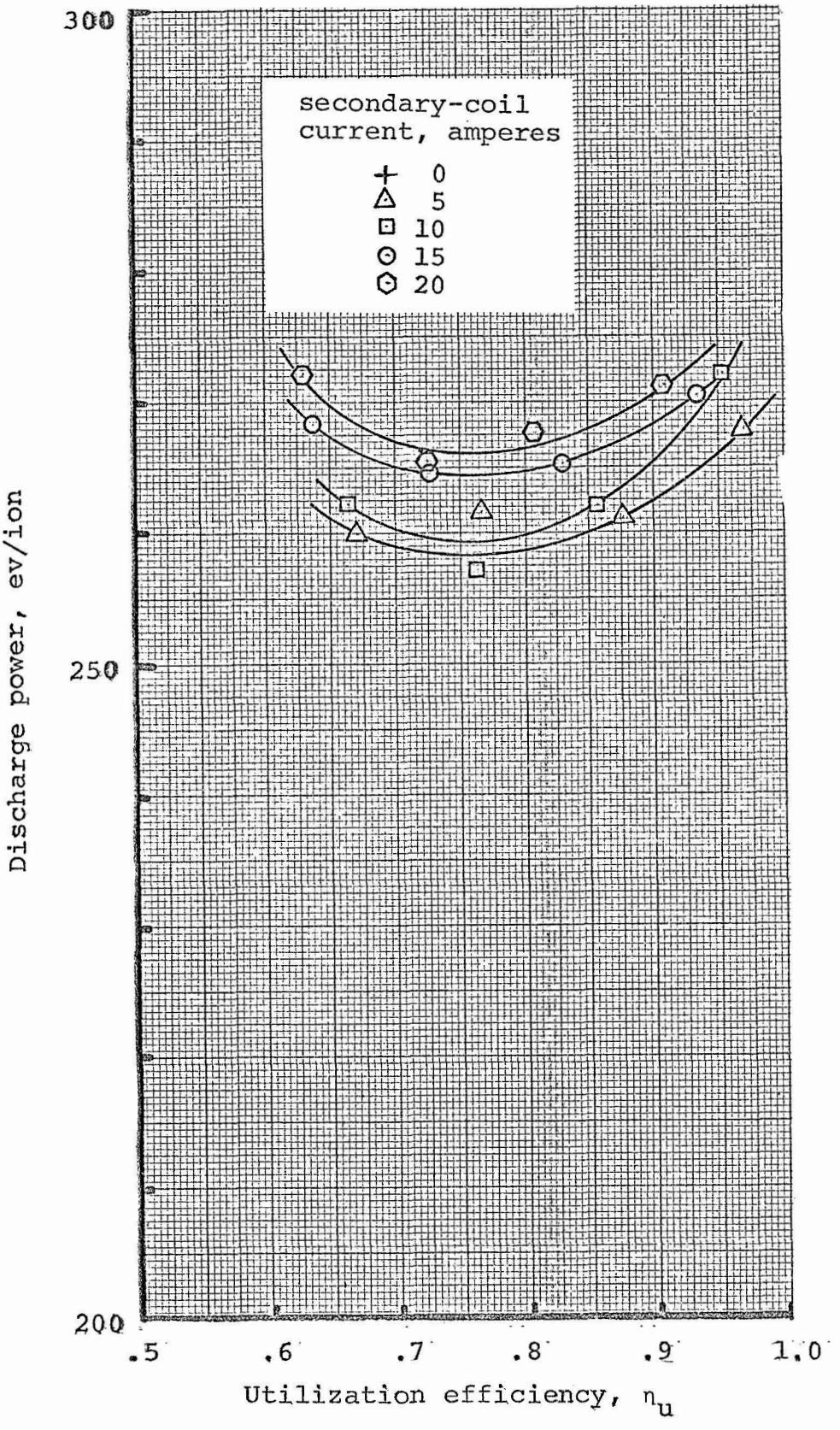

FIG. 17 - (cont.)

(c) secondary-coil current normal direction; single-solenoid coil current 5 amperes aiding main magnetic field.

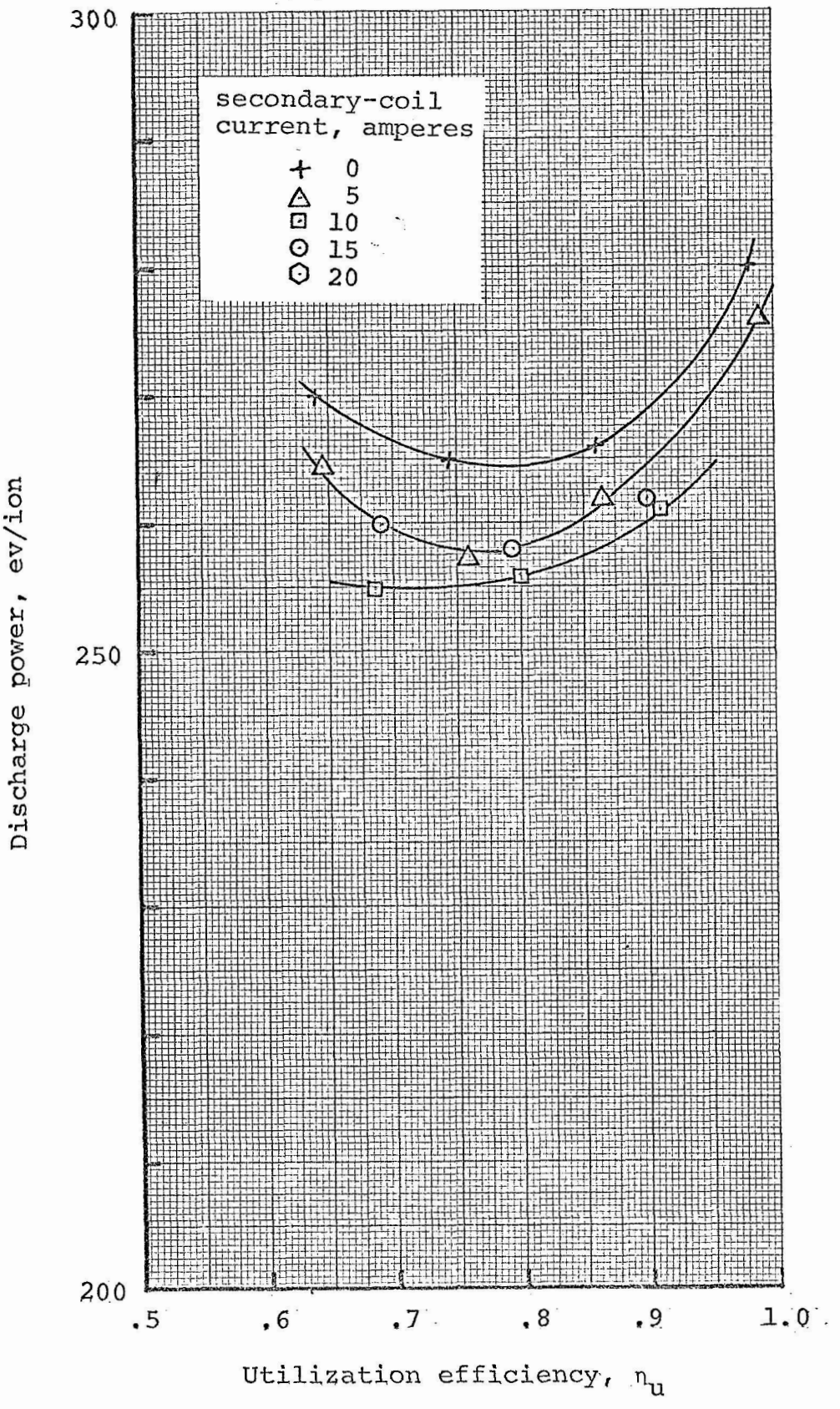

FIG. 17 - (cont.)

(d) secondary-coil current reversed direction; single-solenoid coil current, 5 amperes aiding main magnetic field.

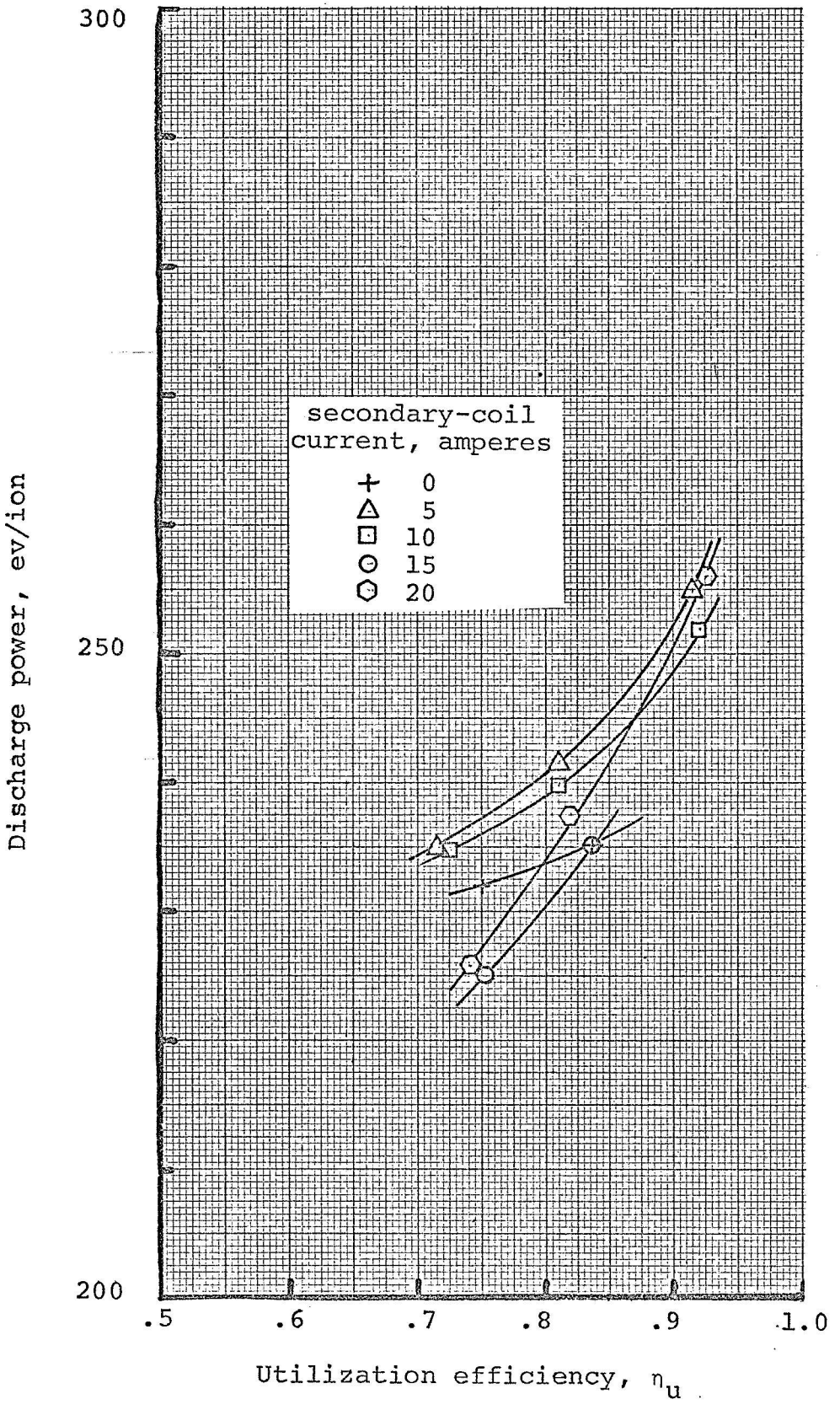

FIG. 17 - (cont.)

(e) secondary-coil current normal direction; single-solenoid coil current, 5 amperes opposing main field.

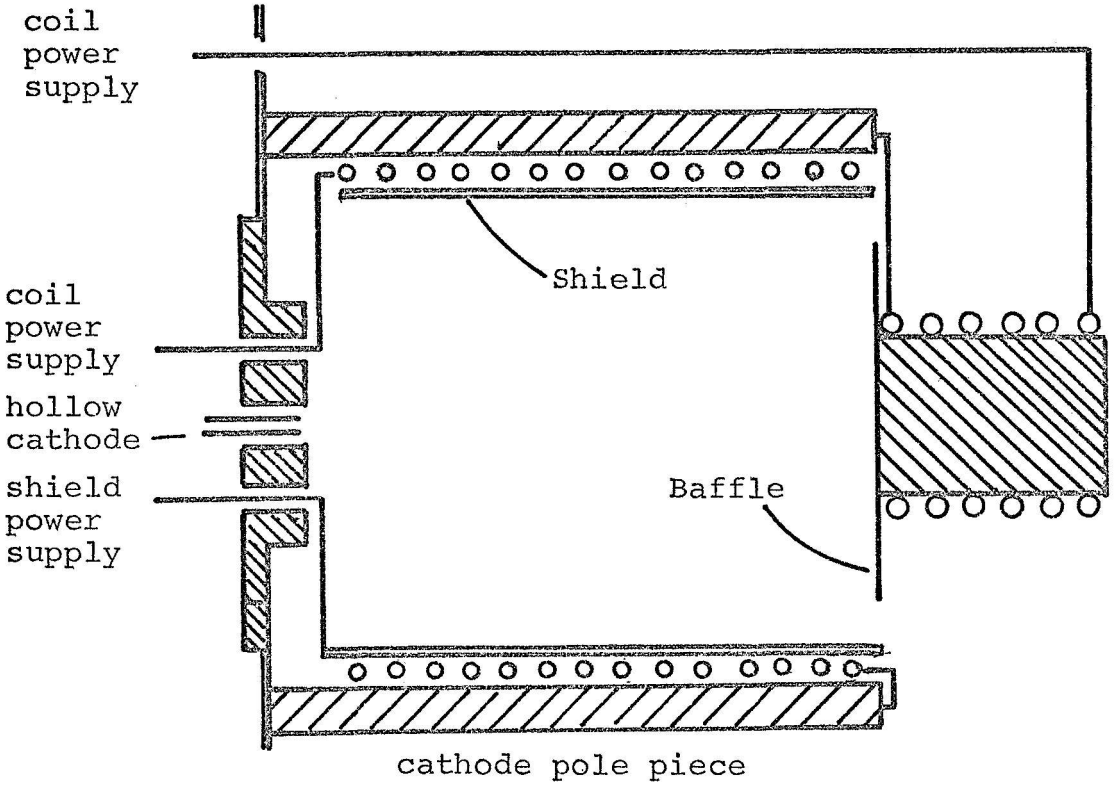

FIG. 18 - Cathode solenoid configuration with coil on baffle. Baffle coil at cathode potential. Shield diameter, 5-cm; shield length, 4.5-cm; baffle diameter, 4.25-cm; baffle coil diameter, 2-cm; baffle length, 4-cm; pole piece diameter, 6.3-cm; pole piece length, 6.3-cm; main coil, 420 turns/meter; baffle coil, 320 turns/meter.

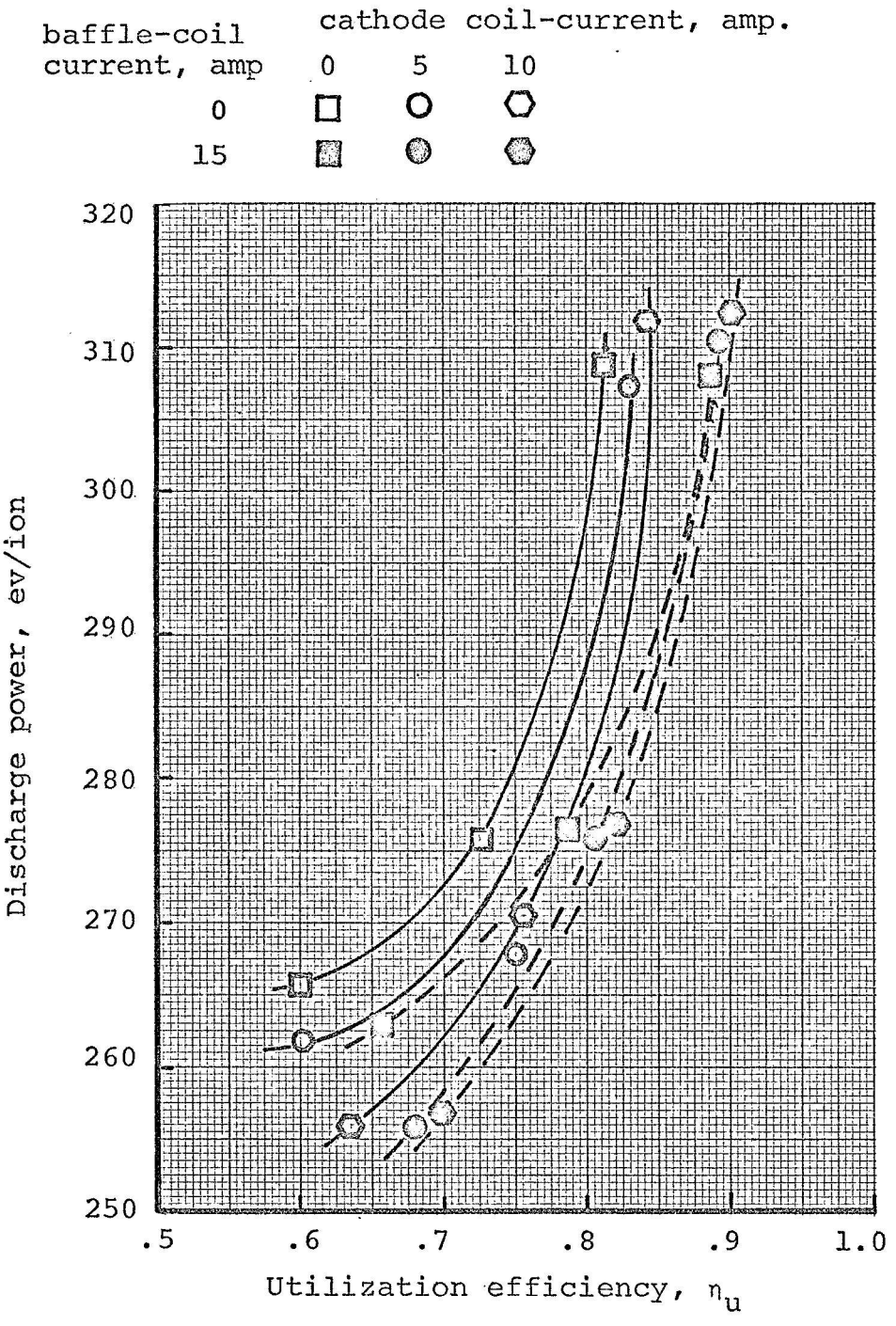

(a) variation of cathode-coil current (data taken Feb. 15, 1970)

FIG. 19 - Discharge power with baffle-coil magnetic field, current in reversed direction. Main magnet current, 1.7 amperes. Ratio of cathode/main flow rates, 0.124. Total mass flow rate, 5.6 gm/hr.

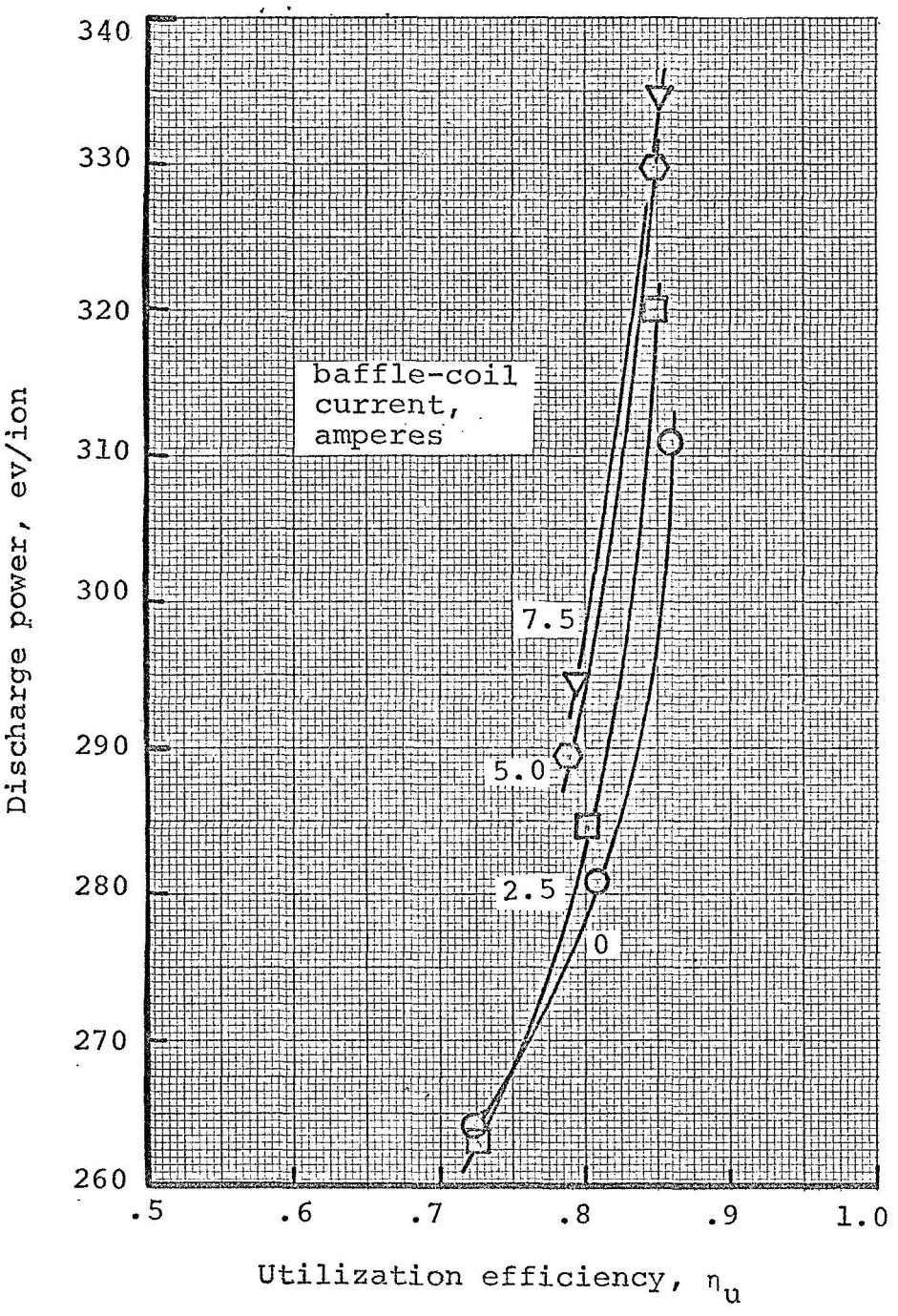

FIG. 19 - (cont.)

(b) cathode-coil current, 0 amperes (data taken later on Feb. 15, 1970)

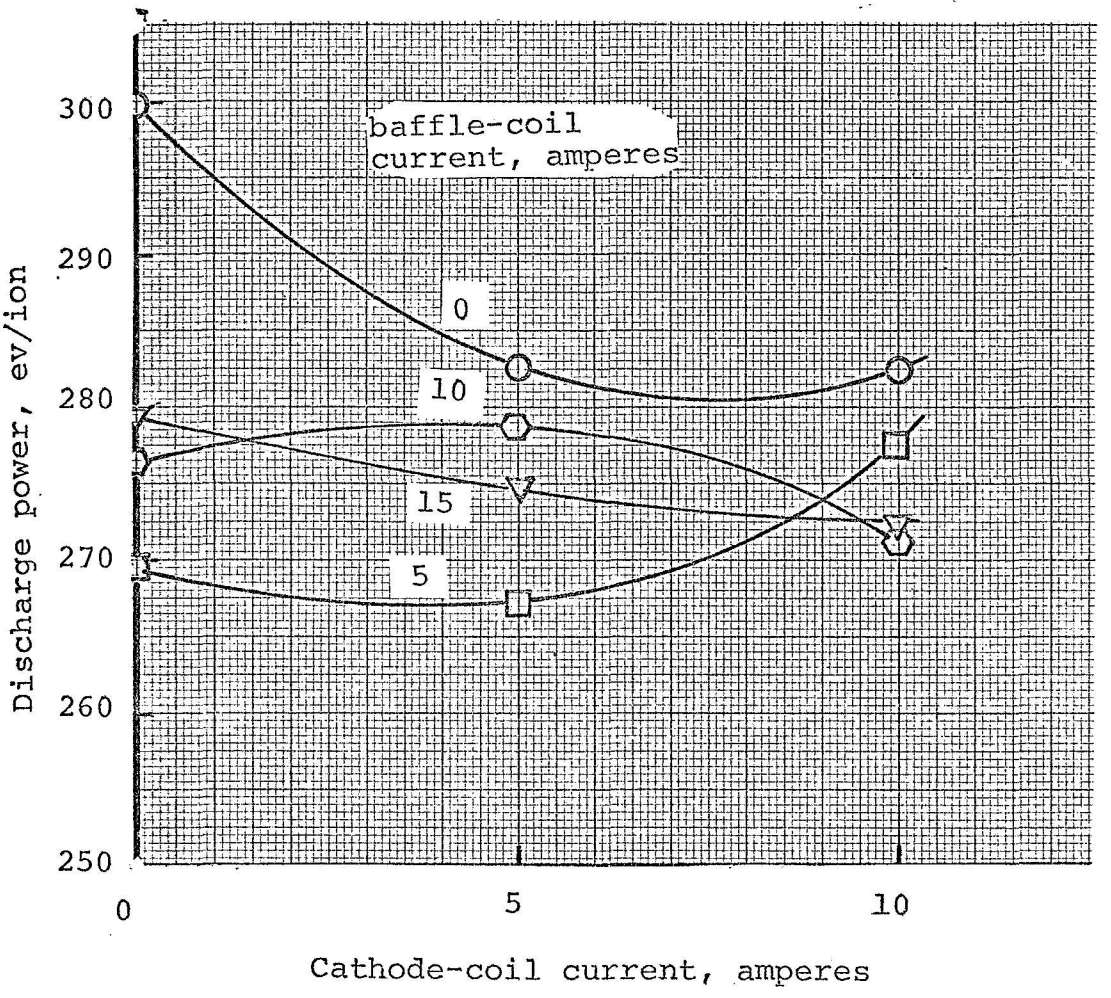

FIG. 19 - (cont.)

(c) utilization efficiency, 80%

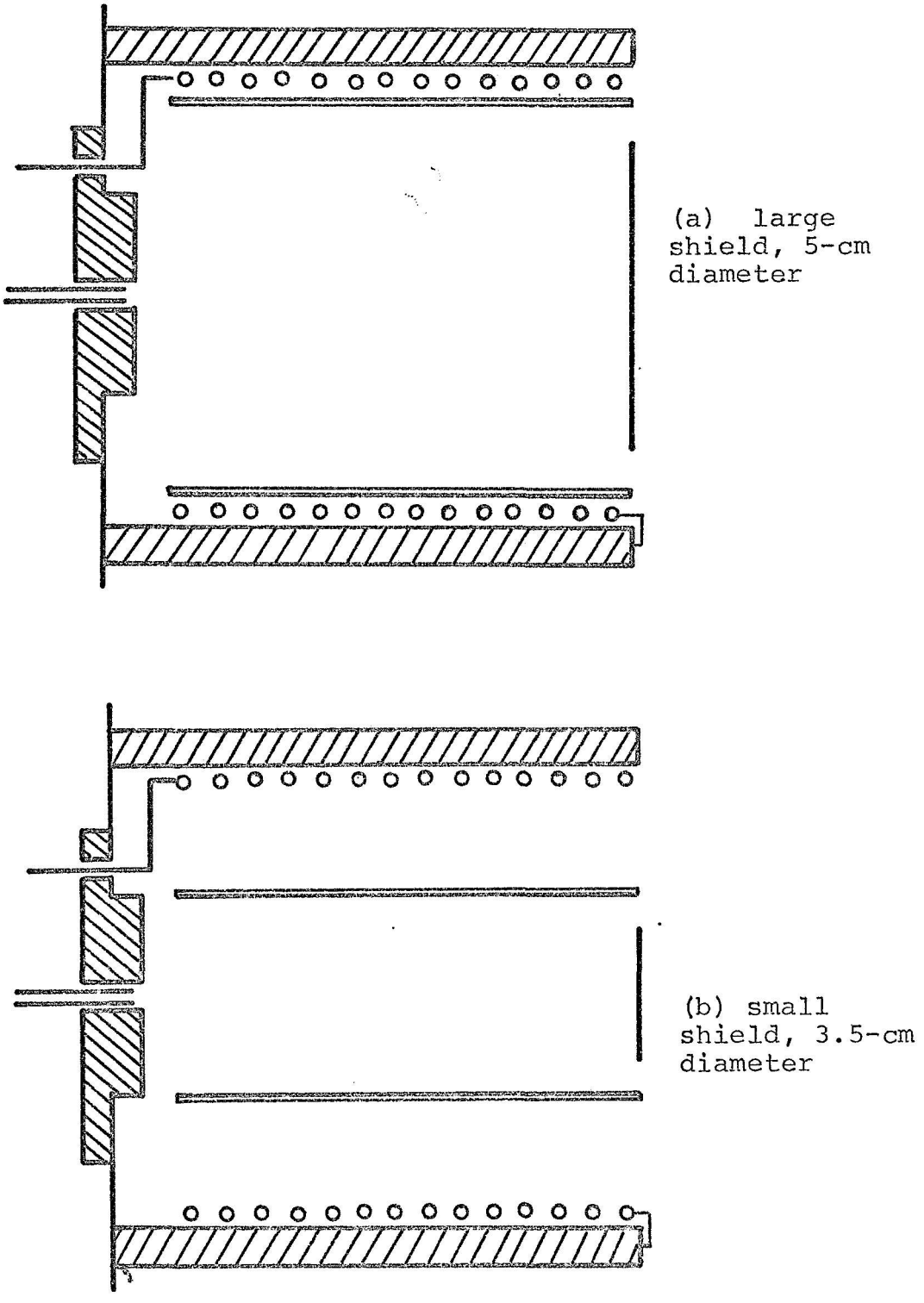

FIG. 20 - Cylindrical shields inside cathode pole piece. Shields and baffle at floating potential.

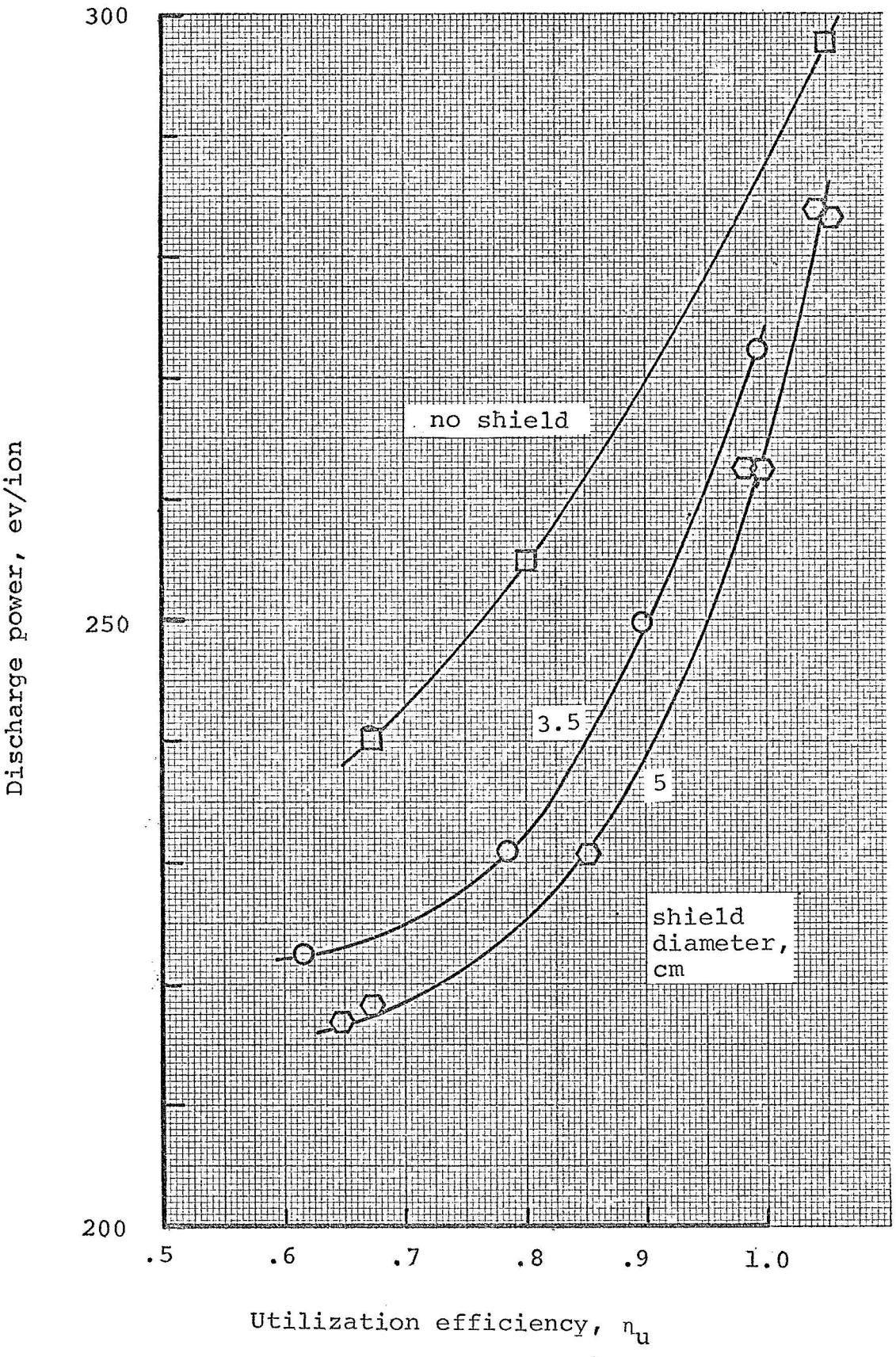

FIG. 21 - Effect of cylindrical shields on discharge power. Total propellant flow rate, 5.5 to 5.7 gm/hr; cathode/main flow with no shield 0.14; cathode/main flow with shield, 0.12; main magnet current, 1.9 ampere; shield at floating potential.

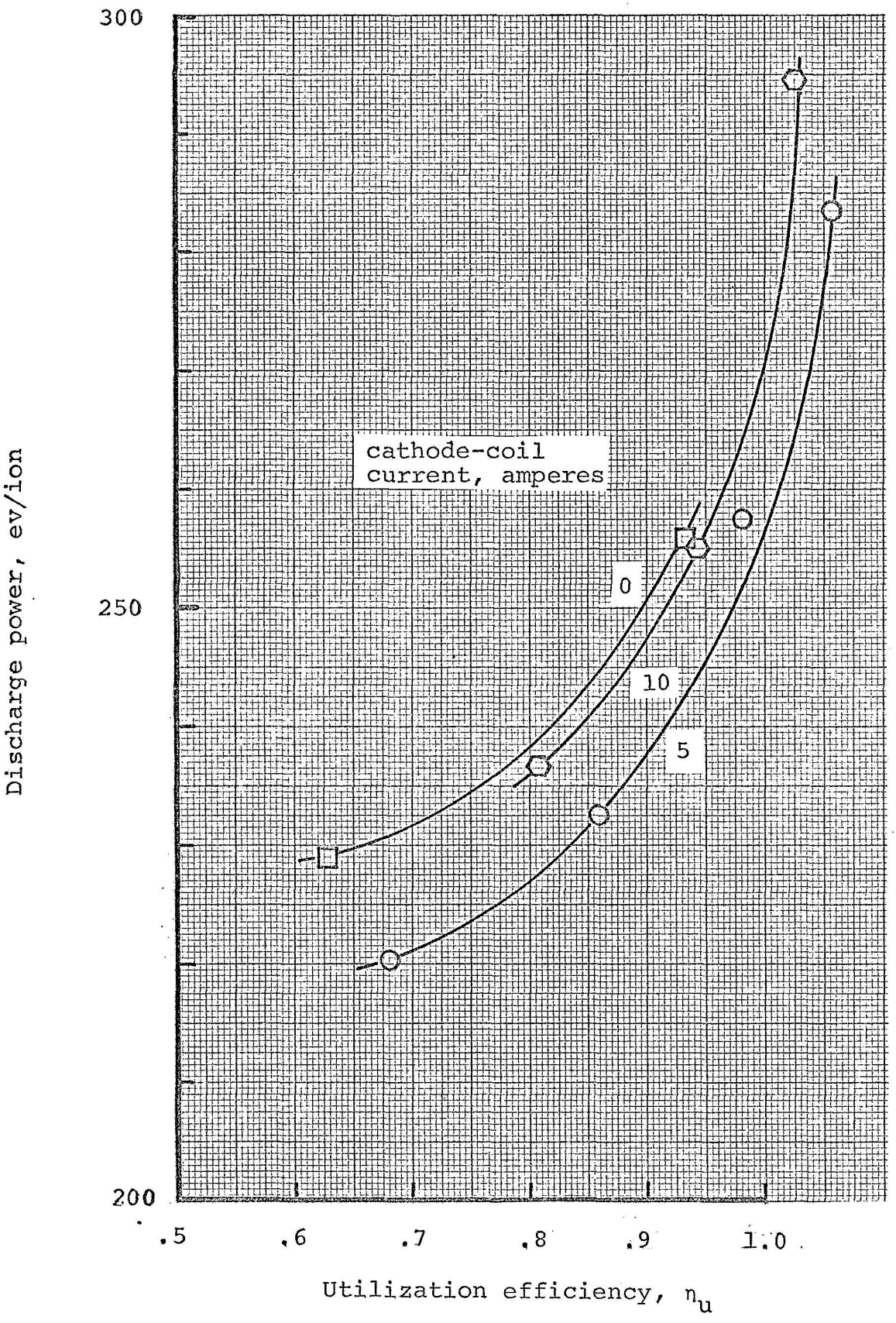

(a) main magnet current, 1.5 ampere

FIG. 22 - Discharge power for single-solenoid cathode magnetic field opposing main field. Large shield and baffle floating; propellant flow rate, 5.7 gm/hr.

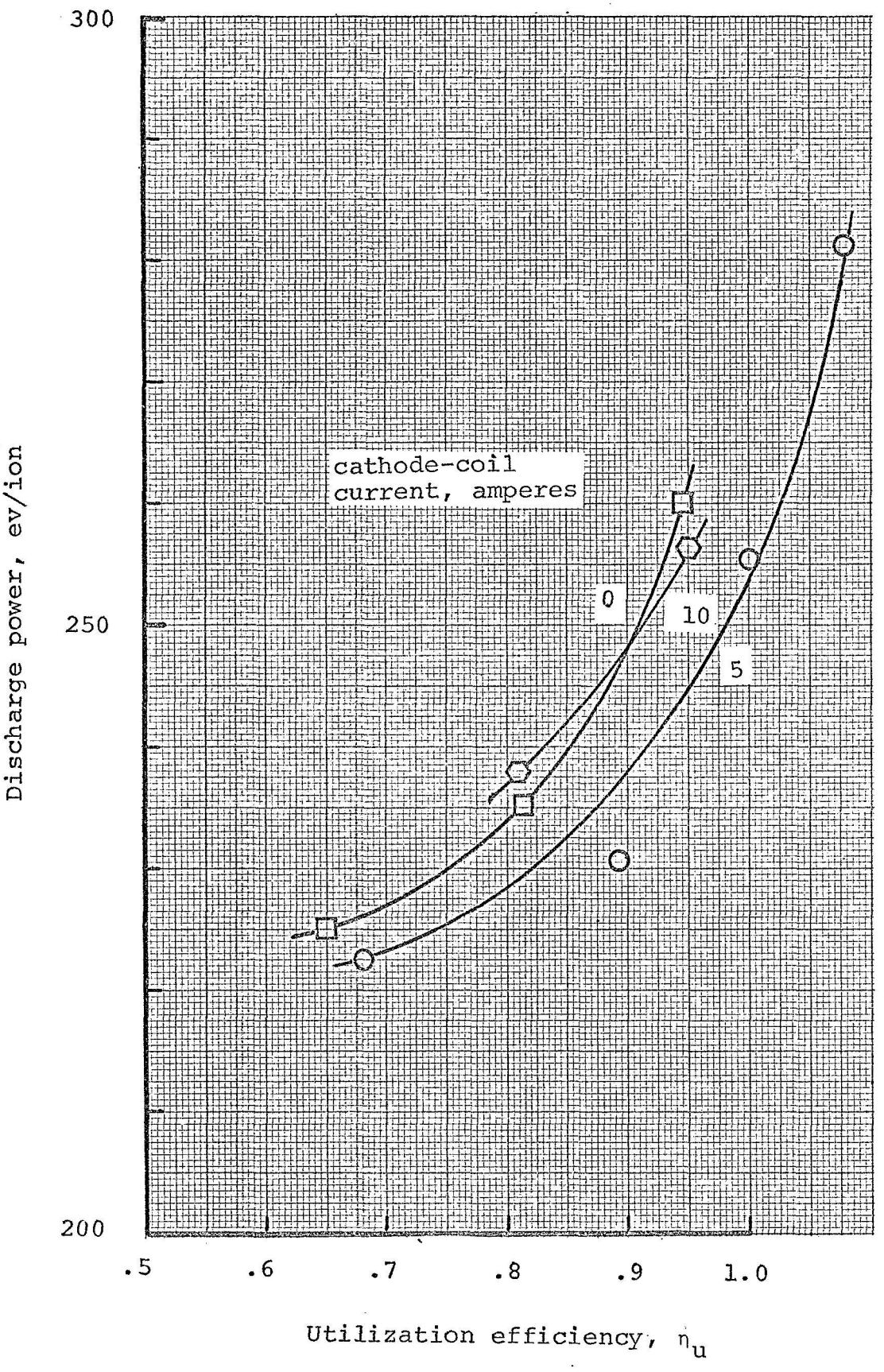

(b) main magnet current, 1.7 ampere

FIG. 22 - (cont.)

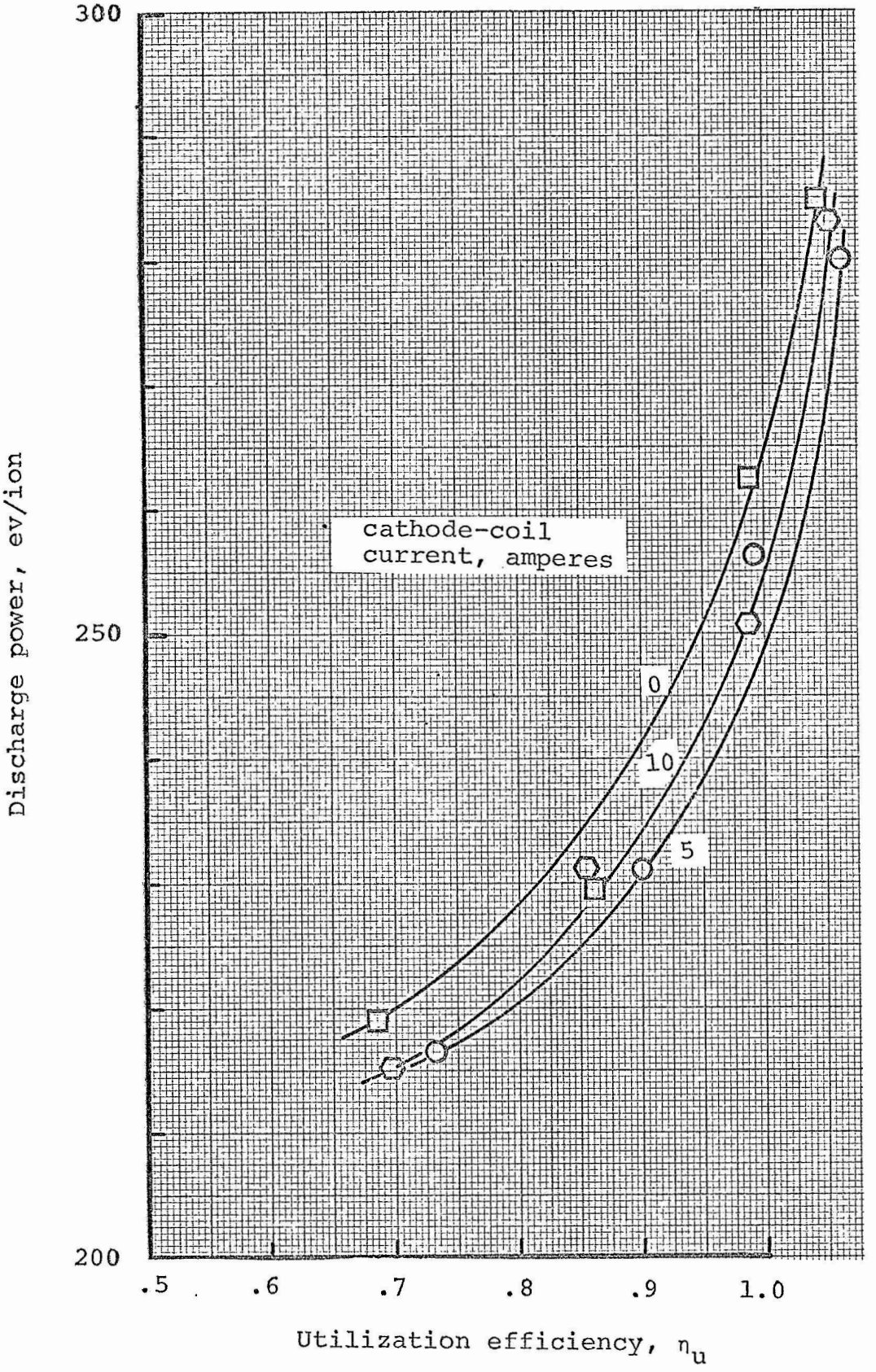

(c) main magnet current, 1.9 amperes

FIG. 22 - (cont.)

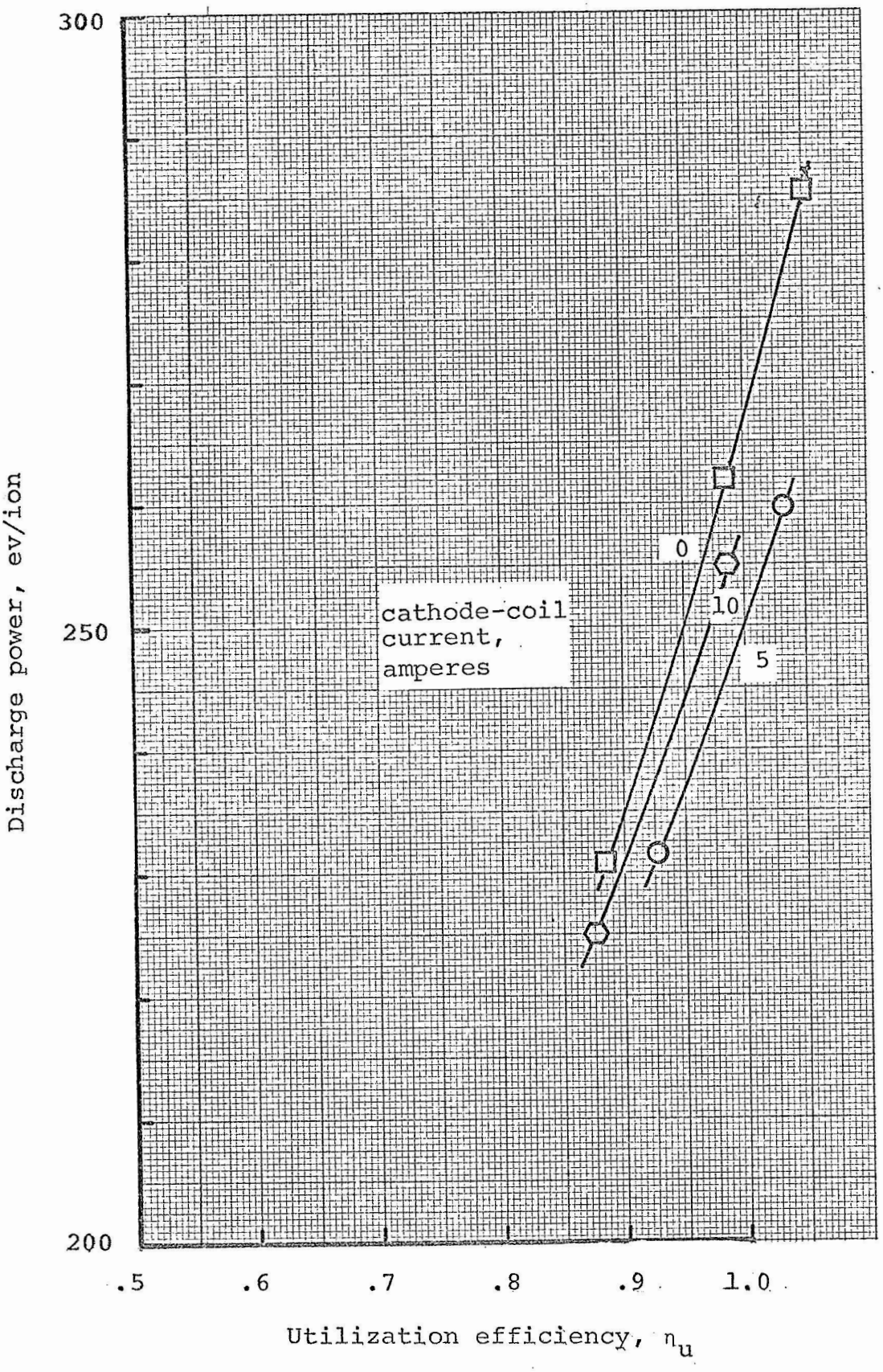

(d) main magnet current, 2.1 amperes

FIG. 22 - (cont.)

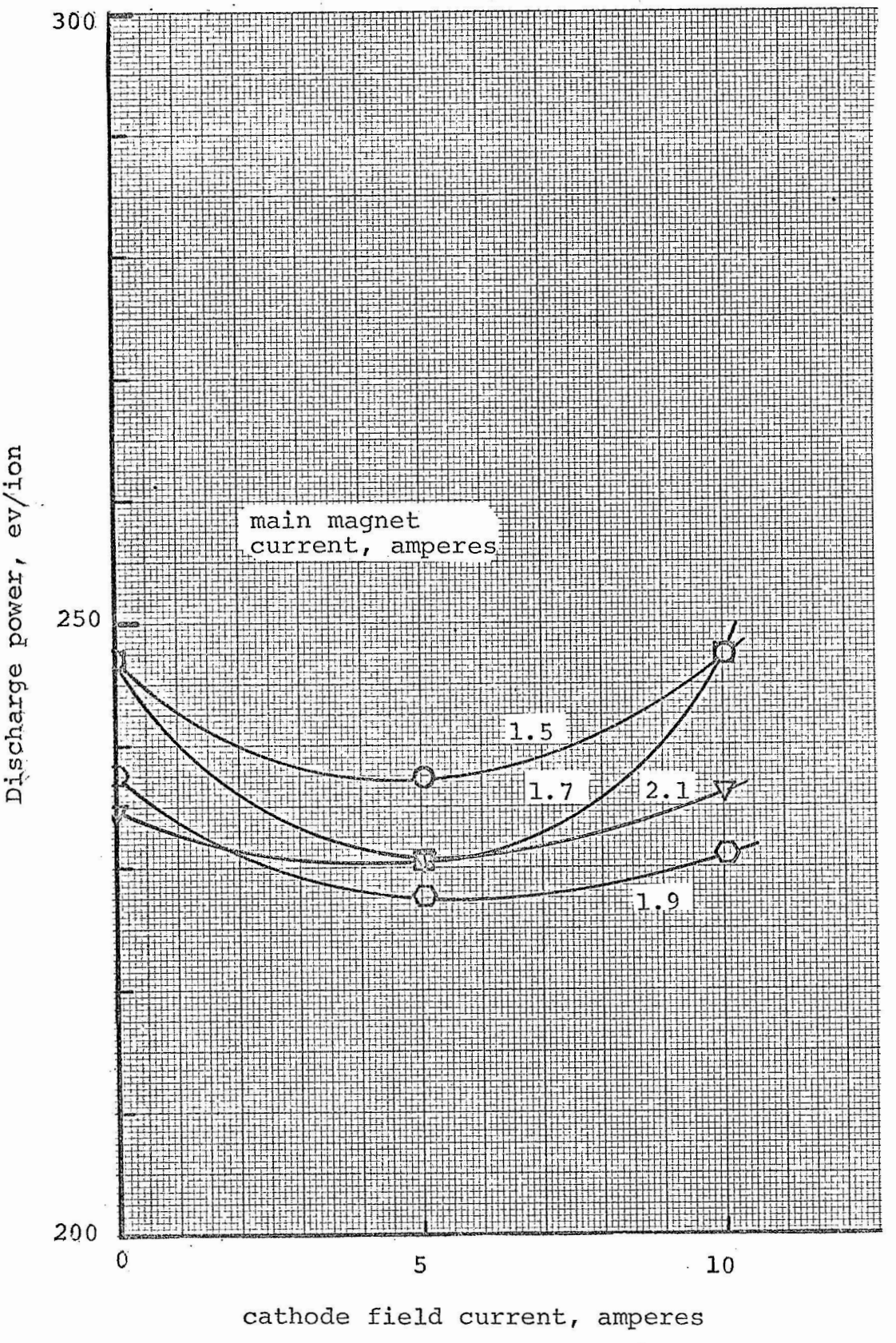

FIG. 23 - Effect of cathode field on discharge power. Shield and Baffle floating; utilization efficiency, 90%.

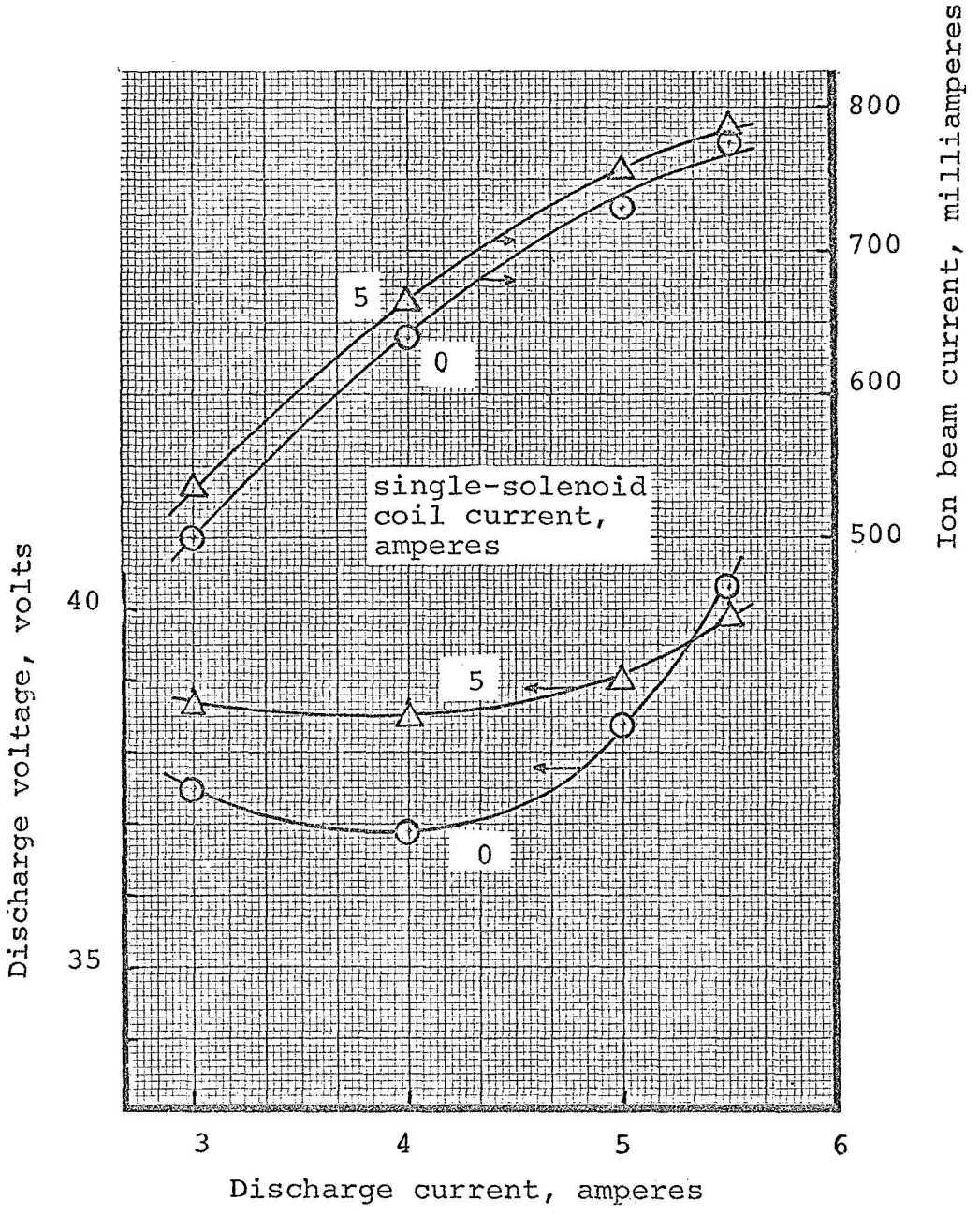

FIG. 24 - Effect of cathode field on discharge power. Shield and baffle at floating potential; main magnet current, 1.9 amperes; single-solenoid current, 5 amperes opposing main magnetic field.

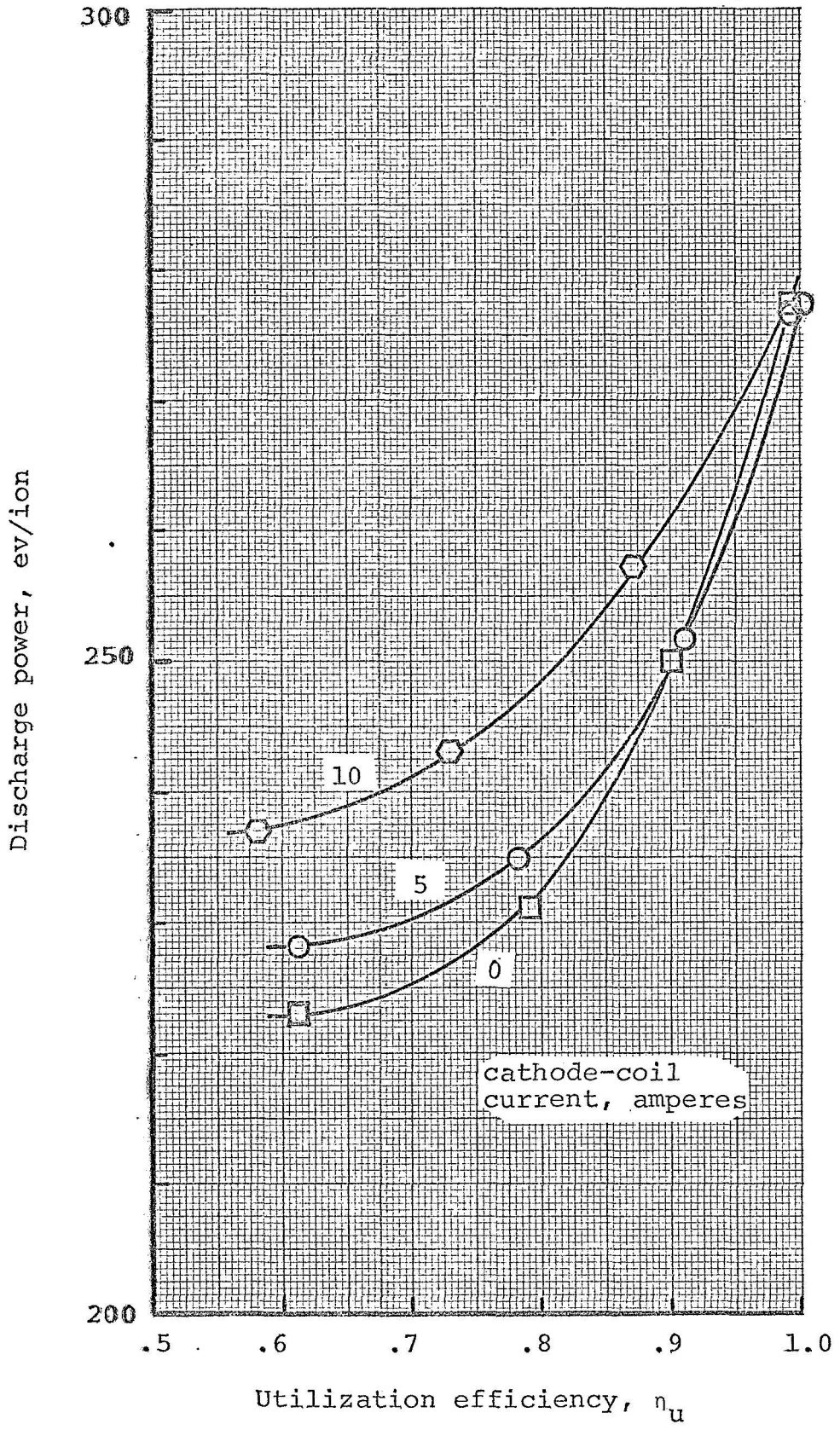

FIG. 25 - Discharge power with small cylindrical shield and single-solenoid cathode coil magnetic field opposing main field. Main magnet current, 1.9 ampere; propellant flow rate, 5.5 gm/hr.

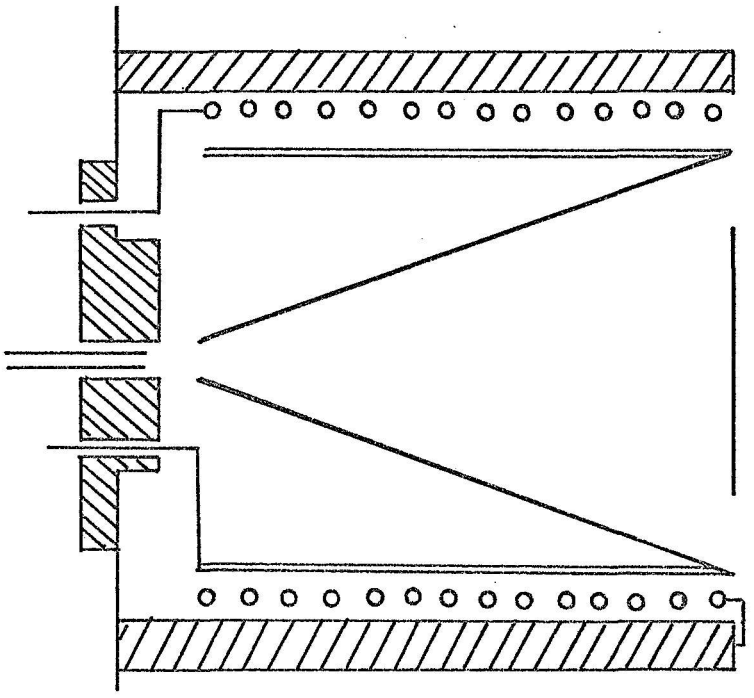

FIG. 26 - Conical shield configuration.

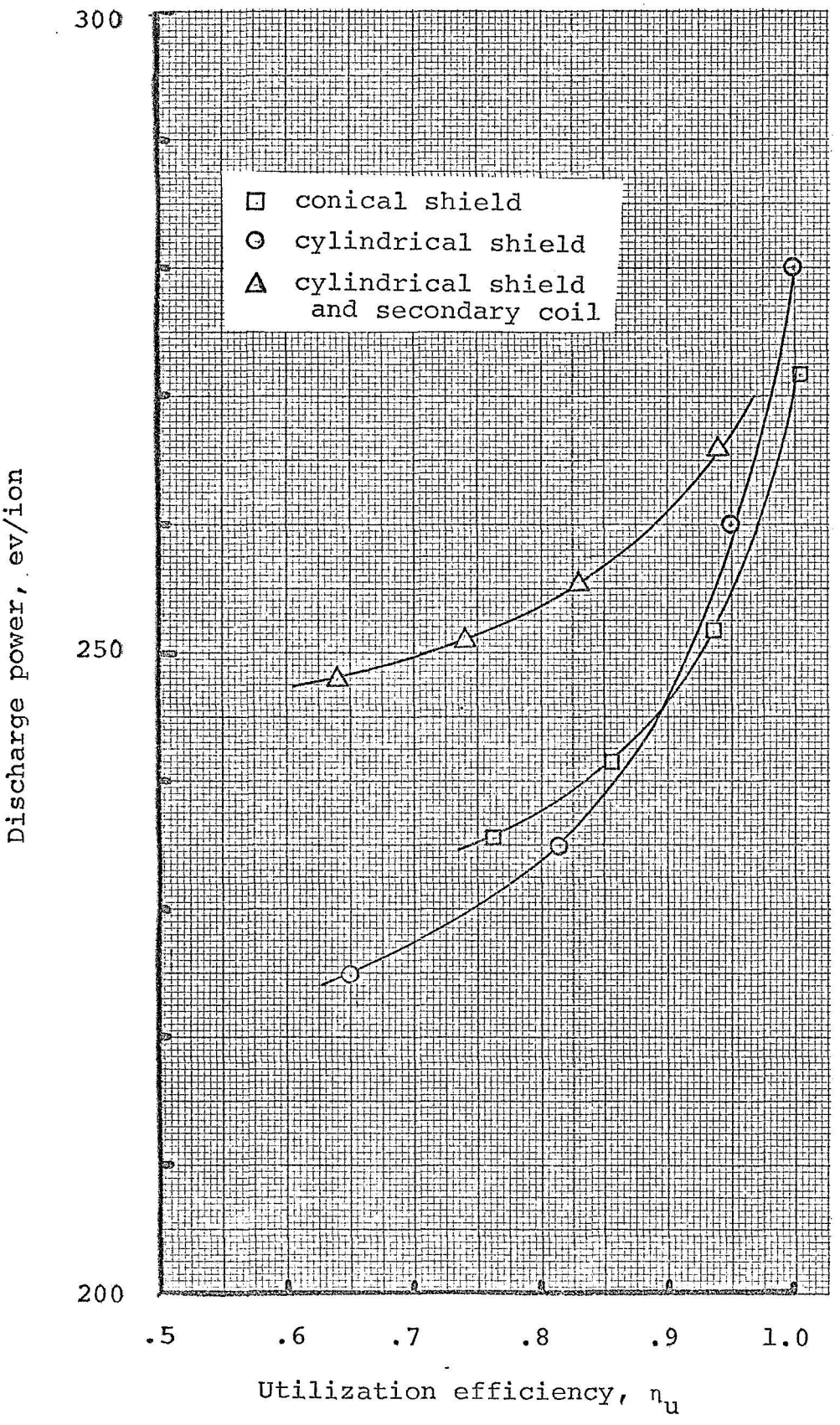

FIG. 27 - Effect of shield shape on discharge power. Main magnet current, 1.7 amperes; single-solenoid coil current, 0 amperes; shields and baffle floating; propellant flow rate 5.5 gm/hr.

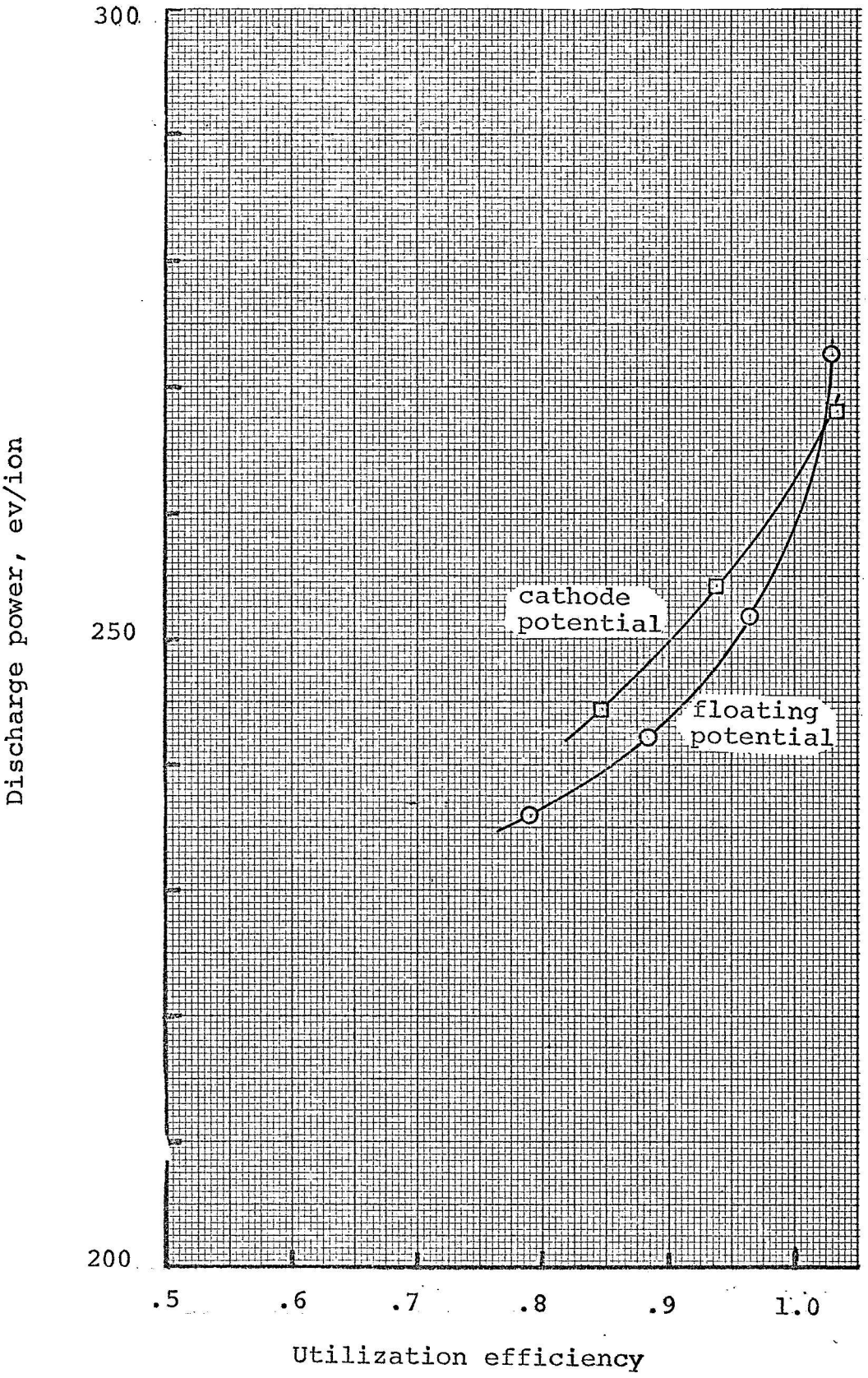

FIG. 28 - Effect of shield potential on discharge power. Main magnet current, 1.7 amperes; single-solenoid coil current, 0 amperes.

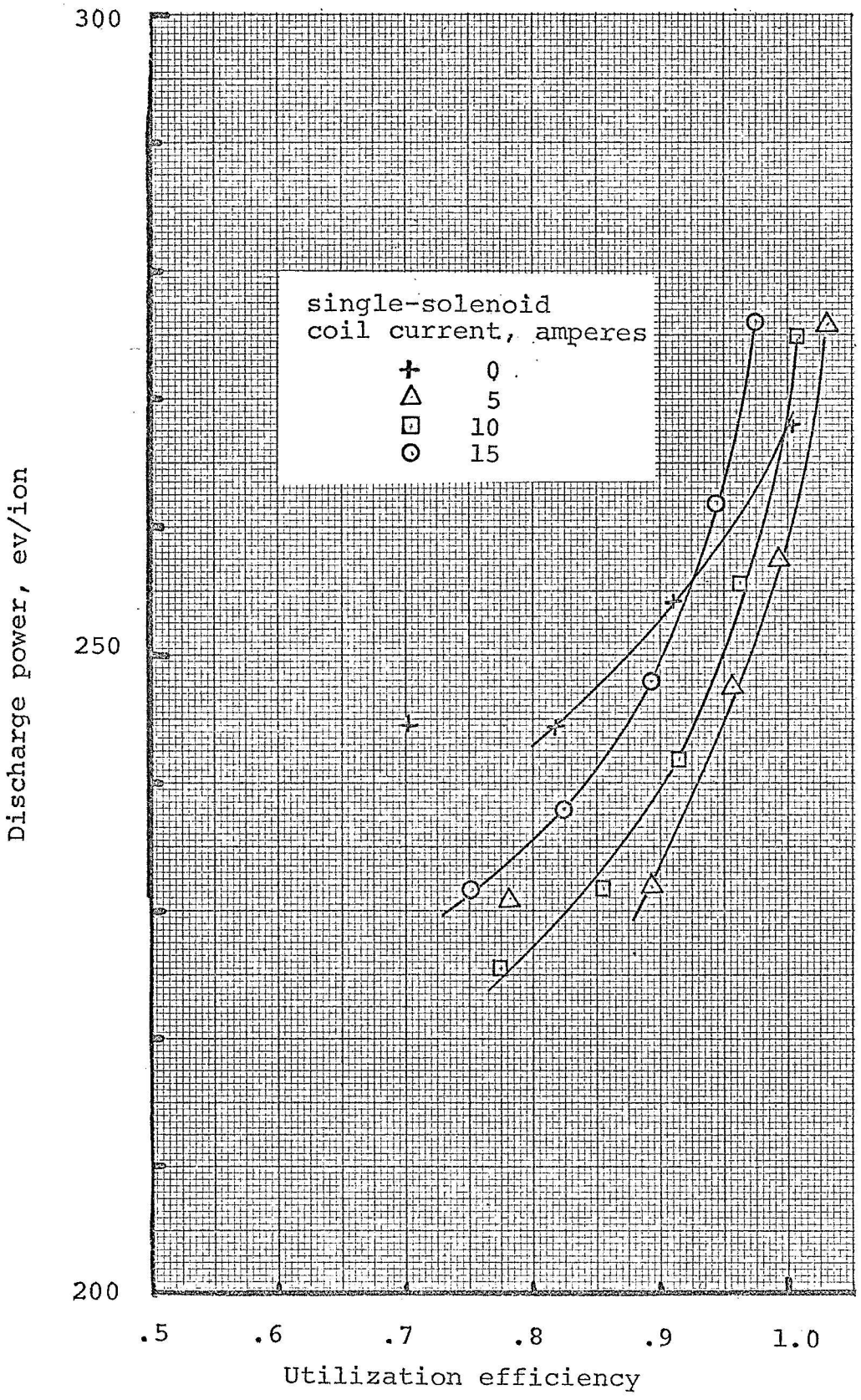

FIG. 29 - Effect of cathode field on discharge power. Cathode field opposing main field. Main magnet current, 1.7 amperes; shields at cathode potential; baffle at floating potential.

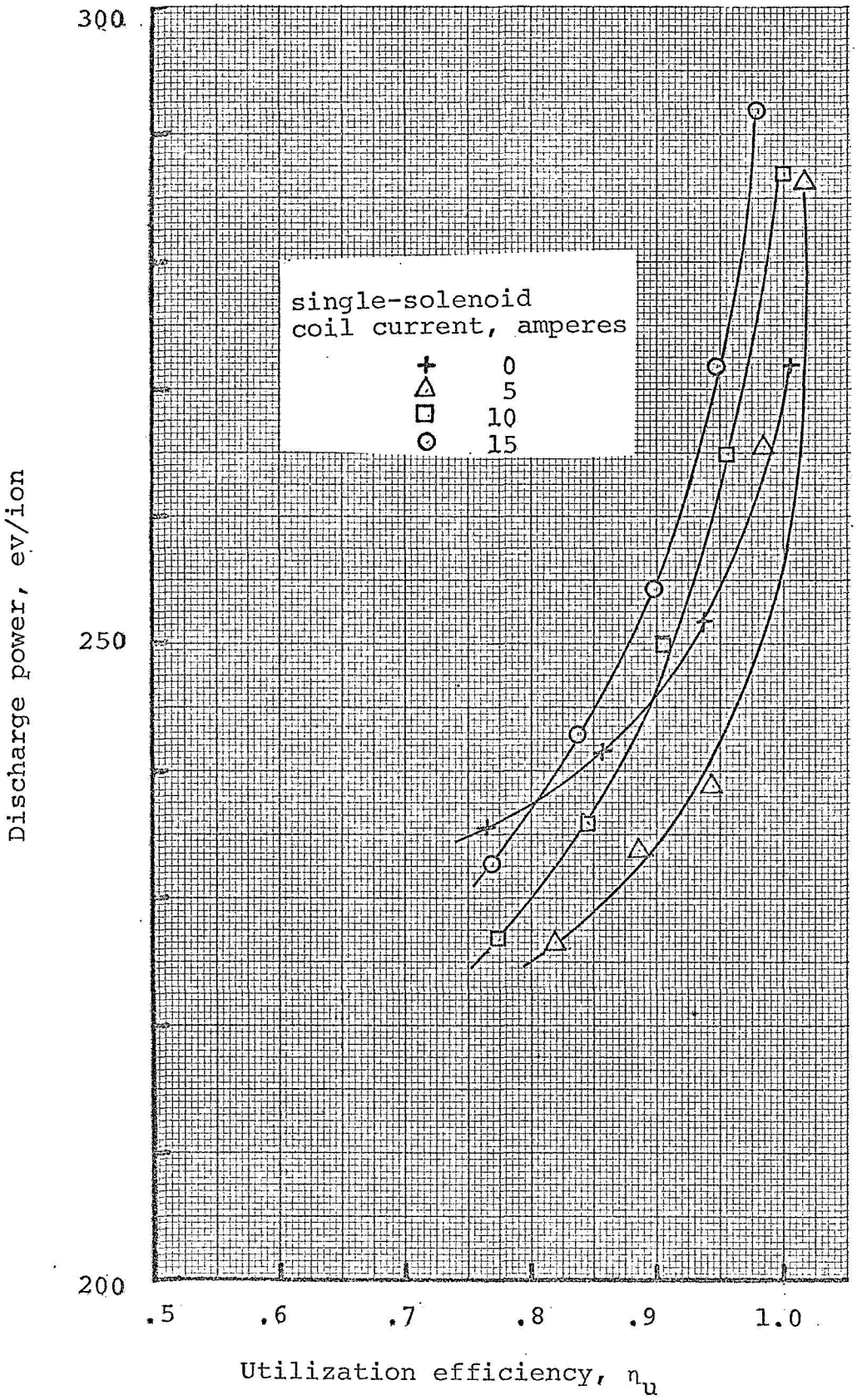

FIG. 30 - Effect of cathode field on discharge power. Cathode field opposing main field. Main magnet current, 1.7 amperes; shields and baffle at floating potential.

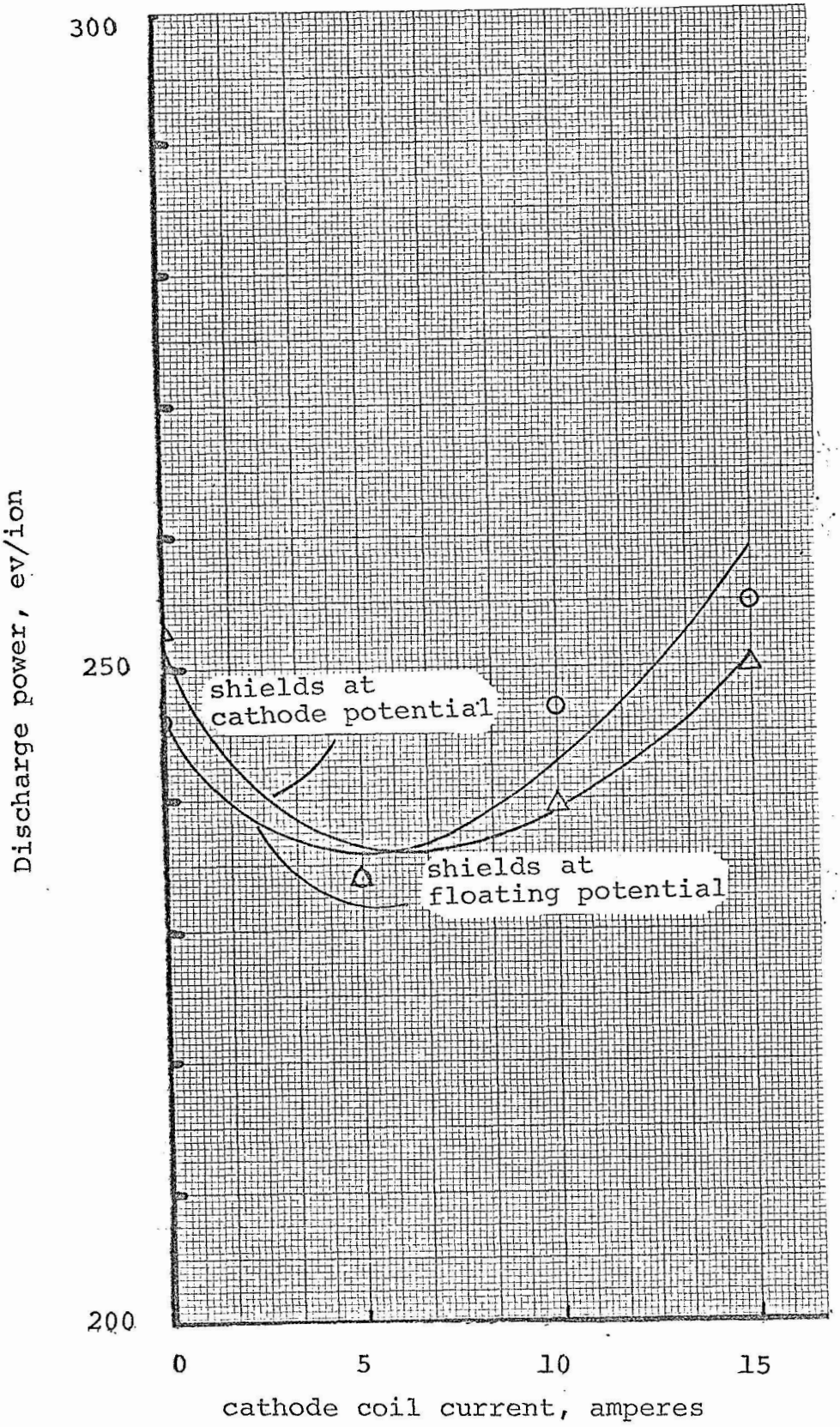

FIG. 31 - Effect of cathode field on discharge power. Cathode field opposing main field. Main magnet current, 1.7 amperes; utilization efficiency, 90%; baffle at floating potential.